HHS Public Access

Author manuscript

J Neurosci Res. Author manuscript; available in PMC 2018 March 01.

Published in final edited form as:

J Neurosci Res. 2017 September ; 95(9): 1871–1887. doi:10.1002/jnr.24024.

Stimulation of Synaptoneurosome Glutamate Release by Monomeric and Fibrillated α-Synuclein

Theodore A. Sarafian[1], **Kaitlyn Littlejohn**[1], **Sarah Yuan**[1], **Charlene Fernandez**[1], **Marianne Cilluffo**[2], **Bon-Kyung Koo**[3], **Julian P. Whitelegge**[1], and **Joseph B. Watson**[1]

[1]Department of Psychiatry and Biobehavioral Sciences, David Geffen School of Medicine, UCLA, Los Angeles, CA

[2]Brain Research Institute, UCLA, Los Angeles, CA

[3]Department of Chemistry and Biochemistry, UCLA, Los Angeles, CA, USA

Abstract

The α-synuclein protein exists *in vivo* in a variety of covalently modified and aggregated forms associated with Parkinson's disease (PD) pathology. However, the specific proteoform structures involved with neuropathological disease mechanisms are not clearly defined. Since α-synuclein plays a role in presynaptic neurotransmitter release, an *in vitro* enzyme-based assay was developed to measure glutamate release from mouse forebrain synaptoneurosomes (SNs) enriched in synaptic endings. Glutamate measurements utilizing SNs from various mouse genotypes (WT, over-expressers, knock-outs) suggested a concentration dependence of α-synuclein on calcium/depolarization-dependent presynaptic glutamate release from forebrain terminals. *In vitro* reconstitution experiments with recombinant human α-synuclein proteoforms including monomers and aggregated forms (fibrils, oligomers) produced further evidence of this functional impact. Notably, brief exogenous applications of fibrillated forms of α-synuclein enhanced SN glutamate release but monomeric forms did not, suggesting preferential membrane penetration and toxicity by the aggregated forms. However, when applied to brain tissue sections just prior to homogenization, both monomeric and fibrillated forms stimulated glutamate release. Immuno-gold and transmission electron microscopy (TEM) detected exogenous fibrillated α-synuclein associated with numerous SN membranous structures including synaptic terminals. Western blots and immuno-gold TEM were consistent with SN internalization of α-synuclein. Additional studies revealed no evidence of gross disruption of SN membrane integrity or glutamate transporter function by exogenous α-synuclein. Overall excitotoxicity, due to enhanced glutamate release in the face of either overexpressed monomeric α-synuclein or extrasynaptic exposure to fibrillated α-

To whom correspondence should be addressed: Joseph B. Watson, Ph.D., Semel Institute for Neuroscience and Human Behavior, Room 58-258B, David Geffen School of Medicine at UCLA, 760 Westwood Plaza, Los Angeles, CA 90095-1759, Phone (310)-825-7587; Fax (310)-206-5060; jwatson@mednet.ucla.edu.

CONFLICT OF INTEREST STATEMENT

We are not aware of any conflicts of interests of any kind by the listed authors, who contributed to this manuscript's collective work.

ROLE OF AUTHORS

All authors had full access to all the data in the study and take responsibility for the integrity and the accuracy of the data analysis. Data, Results, Analysis: Theodore A. Sarafian, Kaitlyn Littlejohn, Sarah Yuan, Charlene Fernandez, Marianne Cilluffo, Bon-Kyung Koo, Julian P. Whitelegge, Joseph B. Watson. Manuscript Writing: Theodore A. Sarafian and Joseph B. Watson

synuclein, should be considered as a potential neuropathological pathway during the progression of PD and other synucleinopathies.

Graphical Abstract

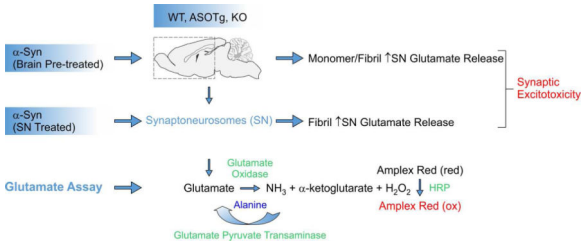

Keywords

α-synuclein; electron microscopy; fibrillated; fluorescence; glutamate oxidase; synaptoneurosome; excitotoxicity; RRIDs: MGI:3617632; IMSR_JAX:000664; IMSR JAX: 100011; MGI:5435401; MGI:2389489; AB_91785; AB_398107; AB_10683386; AB_437779; AB_2629850; AB_1163659; SCR_003210

INTRODUCTION

A current consensus is that α-synuclein is a central toxic protein involved in both familial and sporadic forms of Parkinson's disease (PD), which remains a highly prevalent debilitating neurodegenerative disease (Dauer and Przedborski, 2003; Shulman et al., 2011; Houlden and Singleton, 2012). The α-synuclein protein exists in a variety of aggregated forms including oligomers and fibrils associated with progressive PD pathology (Roberts and Brown, 2015; Villar-Pique et al., 2015), but the toxic species are likely to be a dynamic mix of multiple forms. In light of α-synuclein's function in modulating presynaptic vesicles (Bendor et al., 2013), it is important to understand which proteoforms function at both normal and PD terminals. For example, α-helical α-synuclein monomers and/or oligomers (perhaps tetramers) may normally interact with synaptic vesicle membranes or directly with synaptobrevin in the SNARE complex (Bartels et al., 2011; Wang et al., 2011; Burre et al., 2015; Dettmer et al., 2015). Conversely, cytosolic unfolded monomers (Watson et al., 2009; Fauvet et al., 2012; Sarafian et al., 2013; DeWitt and Rhoades, 2013; Ronzitti et al., 2014) or misfolded β-sheet enriched, amyloid oligomers of α-synuclein may negatively interact with presynaptic entities (Danzer et al., 2007; Diao et al., 2013; Choi et al., 2013; Luth et al., 2014; Spinelli et al., 2014; Chen et al., 2015; Pacheco et al., 2015). Recent reports indicate that fibril forms of α-synuclein also cause cytotoxicity (Mahul-Mellier et al., 2015; Shrivastava et al., 2015), travel between neurons and synapses, and display prion-like abilities by seeding fibril growth in synucleinopathies including PD and multiple systems atrophy (MSA) (Kordower et al., 2008; Li et al., 2008; Volpicelli-Daley et al., 2011; Luk and Lee, 2014; Osterberg et al., 2015; Peelaerts et al., 2015; Prusiner et al., 2015).

Previous reports showed that overexpression of monomeric human α-synuclein can have either positive or negative effects on presynaptic neurotransmitter release, specifically glutamate from corticostriatal terminals (Watson et al., 2009; Bendor et al., 2013). Moreover

the role of aggregated forms, in particular fibrillated forms, on glutamate release has not been clearly defined. To address these issues further, an enzyme-based neurochemical assay was used to measure presynaptic glutamate release in synaptoneurosomes (SNs)(Chang et al., 2012) from multiple mouse genotypes with different amounts of α-synuclein as well as in SNs reconstituted with human α-synuclein proteoforms (monomers, fibrillated). Overall, results showed that exogenous applications of fibrillated forms of α-synuclein preferentially increased mainly calcium/depolarization-dependent glutamate release from SN fractions.

MATERIALS and METHODS

Abbreviations: Analysis of Variance (ANOVA), 8-anilino-1-naphthalenesulfonic acid (ANS), α-synuclein (α-Syn), α-synuclein overexpressing (ASOTg), α-synuclein knock-out (KO, S*nca*$^{-/-}$), bovine serum albumin (BSA), 9-(2,2-dicyanovinyl)julolidine (DCVJ), dithiothreitol (DTT), DL-*threo*-β-benzyloxyaspartic acid (TBOA), ethylenediaminetetraacetic acid (EDTA), ethylene glycol tetraacetic acid (EGTA), guanidinium hydrochloride (GdnCl), horseradish peroxidase (HRP), immunohistochemistry (IHC), Krebs Ringer (KR), modified Krebs-Henseleit (mKRBS), N-α-acetyltransferase complex (NatB), non-amyloid component (NAC), phosphate buffered saline (PBS), polyvinylidene difluoride (PVDF), Research Resource Identifier (RRID), sodium dodecyl sulfate (SDS), soluble NSF (N-ethylmaleimide-sensitive factor) attachment protein receptor (SNARE), synaptoneurosome (SN), SYPRO®Ruby, Thioflavin T (TFT), transmission electron microscopy (TEM), Tris-buffered saline plus 0.05% Tween-20 (TBST), vesicle-associated membrane protein (VAMP), wildtype (WT)

Animals

WT animals included mice in the following genetic backgrounds: C57BL/6 X DBA2 (RRID, MGI:3617632), C57BL/6 (RRID, IMSR_JAX:000664), and B6CBA (RRID, IMSR JAX: 100011). Mice over-expressing human α-synuclein (ASOTg)(C57BL/6 X DBA2)(RRID, MGI:5435401) under the control of the mouse Thy-1 promoter and S*nca*$^{-/-}$ mice lacking α-synuclein expression (KO)(129 X SvEv) (RRID, MGI:2389489) were generated previously (Cabin et al., 2002; Rockenstein et al., 2002; Fleming et al., 2008). Both male and female mice were used and ranged in age from 2–5 months. Groups of 3–4 animals were maintained in cages on a 12 h light cycle at room temperature (21°C) and were fed food and water *ad libitum*. All efforts were made to minimize the number of animals used. Animals were anesthetized with isofluorane prior to dissecting out forebrain tissue. Forebrain samples were divided into smaller sections depending on the experiment. Studies were carried out according to guidelines of the National Institutes of Health Guide for Care and Use of Laboratory Animals (NIH Publications No.80–23), “Guidelines for the Use of Animals in Neuroscience Research” (Society for Neuroscience), and with approval from the Institutional Animal Care and Use Committee at UCLA.

Reagents/Antibodies

Reagents—Fluorescent probes included 9-(2,2-dicyanovinyl)julolidine (DCVJ), Thioflavin T (TFT), and 8-anilino-1-naphthalenesulfonic acid (ANS) (Sigma-Aldrich, St. Louis, MO). DL-*threo*-β-benzyloxyaspartic acid (TBOA) (Tocris Bioscience, Bristol, UK)

was used for glutamate transporter inhibition. An Amplex® Red Glutamic Acid/Glutamate Oxidase Kit Assay was used for glutamate measurements (ThermoFisher Scientific/ Invitrogen, Grand Island, NY).

Antibodies—Both a primary rabbit polyclonal antibody raised against human α-synuclein (aa 111–131immunogen, 1:10,000 dilution, AB5308, EMD/Millipore, Temecula, CA) (RRID:AB_91785) and a mouse monoclonal antibody raised against rat α-synuclein (aa 15–123 immunogen, 1:2000 dilution, Clone 42, BD Transduction Laboratories™, San Jose, CA) (RRID: AB_398107) were used. Secondary antibodies were: goat anti-rabbit (RRID: AB_10683386) or anti-mouse (RRID: AB_437779) conjugated to horseradish peroxidase (HRP, 1:5000–1:10,000 dilution)(CalBiochem/EMD-Millipore, San Diego, CA) for Western immunoblotting. The rabbit polyclonal antibody raised against human α-synuclein was used as primary (1:1000) and anti-rabbit IgG conjugated to 10 nm gold (1:20, #25705, Aurion/ Electron Microscopy Sciences Hatfield, PA)(RRID: AB_2629850) was used as secondary for immuno-gold experiments. A non-immune rabbit IgG fraction served as a negative primary control (#I5006, Sigma-Aldrich, St. Louis, MO)(RRID: AB_1163659) for immuno-gold experiments.

Recombinant Proteins

Human α-synuclein proteins (full-length 1–140aa ± NH_2-terminal acetylation; truncated 1–95aa ± NH_2-terminal acetylation) were produced in the UCLA-DOE Protein Expression Technology Center. A full-length NH_2-terminal acetylated human α-synuclein protein was also prepared by GenScript (Piscataway, NJ). The native (non-acetylated) full-length protein was expressed from an α-synuclein (SNCA, Genbank Accession ID #6622) DNA construct in the pRK172 plasmid and purified as previously described (Der-Sarkissian et al., 2003) with the following changes: a single ion exchange chromatography step was performed using a Q-sepharose column (HiTrap Q-sepharose; GE Healthcare Life Sciences, Pittsburgh, PA) and the protein was subsequently further purified by size exclusion chromatography with a HiPrep Sephacryl S-100 HR column (GE Healthcare Life Sciences) equilibrated in storage buffer (20 mM Tris pH 8.0, 100 mM NaCl, 1 mM DTT, 1 mM EDTA). NH_2-terminally acetylated α-synuclein was produced in *E. coli* BL21 (DE3) by co-expression of native α-synuclein, from the pRK172 plasmid, with the yeast N-α-acetyltransferase complex (NatB) encoded on the pNatB plasmid (NAA25, Genbank Accession ID# 80018) (Johnson et al., 2010). Bacterial cell growth and purification of acetylated α-synuclein used the same procedures as for native α-synuclein. For each preparation, monomeric α-synuclein was identified mostly as a single 14–16 kDa polypeptide band in pooled S-100 fractions resolved on SDS-PAGE gels by staining with either Coomassie Blue or SYPRO®Ruby and also immunostaining using an α-synuclein antibody. Mass spectrometry was also used to confirm the correct molecular weight of the full-length protein (Sarafian et al., 2013).

A truncated α-synuclein construct (α-Syn-1–95aa) was generated by PCR-amplification of the DNA sequence encoding amino acids 1–95 of α-synuclein using the following primers: Syn.Met1.For.(5'TTTAAGAAGGAGATATACATATGGATGTATTCATGAAAGGACTTTC) Syn.Val95.Rev.

(5'GCAGCCGGATCGGAATTCAAGCTTTTAGACAAAGCCAGTGGCTGC T) with the reverse primer encoding a stop codon after the codon for Val-95 of the α-synuclein sequence. The PCR product was digested with NdeI and HindIII and ligated into the pRK172 vector backbone, which had been digested with the same restriction enzymes (all enzymes from New England Biolabs, Ipswich, MA). The truncated DNA sequence was verified by DNA sequencing (Genewiz, South Plainfield, NJ). The native and NH_2-terminally acetylated truncated proteins were prepared using the same procedures as for full-length α-synuclein. For each preparation, truncated α-synuclein was confirmed as 10–12 kDa polypeptide band on SDS-PAGE gels by Coomassie or SYPRO®Ruby staining.

Protein Fibrillation

Recombinant α-synuclein proteins were fibrillated by modification of previous methods (Martinez et al., 2007; Chattopadhyay et al., 2008). The α-synuclein monomeric protein (40 μM final) was added to 96-well plates containing either 5 mM potassium phosphate buffer (pH 7.0)/100 mM guanidinium hydrochloride (GdnCl) or 10 mM Tris-HCl pH 7.4/100 mM NaCl. A Teflon bead (0.8 μm) was added to each well and solutions were shaken for up to 72 hrs at 37° C and 300 rpm in a Fluoroskan Ascent FL plate reader. Fluorescence was measured using 2 μM TFT, 8 μM DCVJ, or 8 μM ANS as probes at 2 hr intervals to monitor aggregation. In some cases, fibrillated samples were centrifuged at 12,000 × *g* for 10 min to generate pellet and supernatant fractions.

Protein Assay

Protein concentration was assayed using a Coomassie Blue G-250 Bio-Rad assay as described (Sarafian et al., 2013). Concentrations were calculated using BSA standards.

SDS-PAGE and Native-PAGE/Immunoblotting

The α-synuclein proteoforms (monomers, aggregates) were analyzed by SDS-PAGE using 12% acrylamide gels and a Bio-Rad Mini PROTEAN tetra system as described (Sarafian et al., 2013). For analysis of higher order fibrillated forms, stacking gels were included in Western immunoblot analyses. For Native-PAGE, gels contained 5% acrylamide and lacked SDS. Sample buffers also lacked SDS and were not heated prior to electrophoresis. Gels were transferred onto PVDF membranes, blocked with 5% nonfat dry milk in Tris-buffered saline plus 0.05% Tween-20 (TBST), and stained with anti-α-synuclein (rabbit polyclonal, 1:10,000 or mouse monoclonal, 1:2,000) followed by the appropriate HRP-conjugated secondary antibody. Membranes were stained with ECL Plus reagent (GE Healthcare) and analyzed with a GE 9400 Typhoon Scanner using fluorescence mode.

Synaptoneurosome Fractionation and α-Synuclein Treatment

SNs were prepared from freshly dissected forebrains (mostly cortex and striatum)(~ 100–200 mg wet weight) of WT, ASOTg, or α-synuclein KO mice in Ca^{2+}-free, modified Krebs-Henseleit (mKRBS) buffer pH 7.4 using homogenization and sequential filtrations as described previously (Chang et al., 2012). Final SN pellets were resuspended in 2 ml Ca^{2+}-free mKRBS. For exogenous α-synuclein exposures (SN Treated), either monomeric or fibrillated α-synuclein (0.5–2.0 μg) was added to 100 μl of final SN suspension (5–20 μg/ml,

0.35–1.4 μM). Histone Type II-AS was used as a control protein. Samples were kept at room temperature for 10 min prior to glutamate release assays. For brain pre-treatment studies (Brain Pre-Treated), the same proteins (15–25 μg) were added to the starting brain tissue (50–100 mg wet weight) prior to the homogenization step to facilitate internalization of proteins during membrane disruption and resealing within vesicularized structures including SNs (see Fig. 1). Since greater than 95% of the total protein is lost during the SN preparation (see Johnson et al., 1997), the final SN pellets contained at most 1–2 μg of each internalized α-synuclein proteoform. This assumed complete SN uptake, so the final α-synuclein is likely much lower.

Trypsin Digestion of α-Synuclein Incubated with SNs

Full-length monomeric α-synuclein or truncated α-synuclein 1–95 protein was added either after the final SN fractionation (0.5 μg protein, SN Treated) or prior to tissue homogenization and SN fractionation (30 μg protein, Brain Pre-treated). SNs were then untreated or treated with trypsin (2 μg/ml) for 5 min followed by addition of 40 μM soybean trypsin inhibitor (2 min) and resolved by Western immunoblotting. The α-synuclein protein alone served as a positive control for maximal trypsin digestion. The SNs prepared from KO mice were used to eliminate interference from endogenous mouse synuclein.

Electron Microscopy

Negative staining of recombinant proteins—Purified α-synuclein proteoforms (monomers or aggregates) were processed for transmission electron microscopy (TEM) as described (Tsang et al., 2011; Roychaudhuri et al., 2013). Briefly, each sample (2 μl) containing 40 μM fibrillated α-synuclein was deposited on freshly glow-discharged carbon/formvar coated grids, fixed with 2% glutaraldehyde and stained with 2% uranyl acetate. Each grid was then examined at 60KV on a JEOL 100CX electron microscope. Qualitative observations were made with three separate batches of fibrillated recombinant α-synuclein proteins.

Immunohistochemistry (IHC) staining of recombinant proteins—Prior to SN plus recombinant protein TEM experiments, IHC was initially optimized for purified recombinant proteins. Purified α-synuclein proteoforms (monomers, fibrillated) were deposited on 200 mesh carbon/formvar Ni grids, briefly fixed in 4% paraformaldhehyde and washed in phosphate buffered saline (PBS). The grids were then stained with anti-α-synuclein antibody (AB5038, EMD/Millipore 1:1000), followed by anti-rabbit IgG-10 nm gold (1:20)(see below). After fixation, the grids were negatively stained with 2% uranyl acetate.

Immuno-gold TEM of SNs plus recombinant proteins—For SNs prepared from pre-treated brains (see Fig. 1), 3 equal-sized sections (200–400 μg) from half a KO forebrain were first homogenized (20 vigorous turns of Teflon-pestle) in mKRBS buffer alone or buffer containing either monomeric native (non-acetylated) α-synuclein (35 μg), or fibrillated native synuclein (25 μg) before final pelleting of SNs by micro-centrifugation at ~1,000 × *g*. For SN Treated experiments, a single SN was prepared from the other half of the same KO forebrain, divided into 3 equal volumes (100 μl each) and incubated with buffer

alone or buffer containing either monomeric native α-synuclein (7 μg), or fibrillated native α-synuclein (7 μg) for 15 minutes at room temperature and then an additional 15 minutes at 37°C. SN pellets were regenerated by micro-centrifugation. All final SN pellets were fixed at room temperature with 0.1% glutaraldehyde/4% paraformaldehyde in Krebs Ringers (KR) buffer for 1–2 hours and stored in PBS plus 0.06% sodium azide at 4°C. The SN pellets were dehydrated in a graded series of ethanol up to 80%, infiltrated with LR White resin overnight (Electron Microscopy Sciences), embedded in gelatin capsules and polymerized overnight at 55°C.

Gold interference color sections (approximately 70 nm) were cut on a TMC ultramicrotome and deposited on 200 mesh nickel grids. The grids were washed with PBS, blocked with 1% bovine serum albumin (BSA)/PBS for 1 hour, and incubated with rabbit anti-α-synuclein antibody (AB5038, 1:1000) either overnight or at room temperature for 2 hours. The grids were then washed multiple times with PBS and incubated with anti-rabbit IgG conjugated to 10 nm gold (1:20) (Sreekumar et al., 2010; Lasser et al., 2012) for 1 hour, washed extensively and fixed with 2% glutaraldehyde for 10 minutes. Non-immune rabbit IgG was used as a control serum. After washing in double-distilled water, the grids were counterstained with saturated uranyl acetate followed by Reynold's lead citrate. Immuno-gold-TEM was repeated in two separate experiments with different KO mice for both brain-pretreated SNs and exogenous SN treated experiments.

Glutamate Assay

Glutamate was measured by glutamate oxidase activity coupled to Amplex Red fluorescence using a modification of the manufacturer's protocol (ThermoFisher Scientific/Invitrogen, Fig. 1)(also see Valencia et al., 2013). An enzyme cocktail (25 μl) containing Amplex Red, glutamate oxidase, glutamate aspartate transaminase and HRP was combined with 25 μl SNs in wells of a 96-well plate. For reconstitution experiments, α-synuclein proteoforms or other control proteins were added to brain tissue prior to the initial homogenization (Brain Pre-treated) or added to the final SN fraction (SN treated) for 10 min. For all glutamate assays requiring recombinant proteins, SNs were made from WT mice. SN samples (100 μl) were treated with either 2 μl H_2O ± 2 mM EGTA (basal) or 40 mM KCl plus 0.5 mM $CaCl_2$ (stimulated) and 25 μl aliquots in triplicate were transferred to a 96-well plate. After transfer of all SN samples, the glutamate assay cocktail was added and the plate was shaken for 10 sec at 300 rpm. The plate was incubated for 30 min at 37° C and red fluorescence (Ex = 535, Em = 585) was measured using either a Cytofluor 2300 (Millipore) or Fluorskan FL Ascent (Thermo Scientific) plate reader after 30 min.

Glutamate concentrations were determined based on glutamate standards in separate wells. For some experiments, absolute values for SN glutamate release were expressed as pmoles per μg protein. There was a dynamic range of basal glutamate values possibly due to variation in SN yield, glutamate oxidase enzyme activity, glutamate standards, and the use of different fluorimeters. However, values were consistently within a similar range for a self-contained set of experiments. For genotype comparisons, data was normalized to % of an absolute average basal value obtained for all WT mice (total of 32) due to constraints on the availability of different mouse backgrounds and genotypes over a period of years.

Membrane Permeabilization

Membrane integrity was assessed using a modified calcein release assay (Tsigelny et al., 2012; Lorenzen et al., 2014). Final SN fractions (SN Treated) were pre-loaded with 4 μM calcein-AM in calcium-free KR buffer for 20 min at room temperature. SNs were then washed twice with 1.0 ml buffer, re-suspended in 1.0 ml buffer, and incubated at 37° C. SN samples were incubated with monomeric and fibrillated forms of α-synuclein, or digitonin (160 μM) as a positive control (Schulz, 1990). Aliquots were removed and centrifuged at the indicated time intervals. Supernatants were assayed for green fluorescence (Ex = 485, Em = 530) using a Cytofluor 2300 plate reader.

Statistical Analysis

Student's *t*-tests were used for two group comparisons. One Way or Two Way ANOVAs were used for comparisons among multiple groups followed by the appropriate post-hoc *t*-tests for pairwise comparisons (Sigma Plot 10/11, RRID: SCR_003210)(also see Watson et al., 2009; Sarafian et al., 2013).

RESULTS

SN Glutamate Assay

Previous reports suggested that overexpression of human α-synuclein can have both positive and negative effects on presynaptic neurotransmitter release, in particular glutamate release from corticostriatal terminals (Liu et al., 2004; Gureviciene et al., 2007; Watson et al., 2009; Bendor et al., 2013; Ronzitti et al., 2014). To further investigate these effects by neurochemical measurements, a scaled down method for fractionating SNs (Chang et al., 2012) was combined with a glutamate assay coupling Amplex Red fluorescence to glutamate oxidase-activity (see Fig. 1).

As shown in Figure 2, reliable measurements of SN glutamate were achievable with the glutamate oxidase assay and a 96-well plate format. In the presence of increasing concentrations (50–1000 picomoles) of glutamate, Amplex fluorescence was stable and constant over a 30 minute period (Fig. 2A). The addition of 0.5 mM $CaCl_2$ and 40 mM KCl to SNs to induce membrane depolarization substantially increased glutamate levels over the same time period relative to controls (KR buffer, EGTA to quench divalent cations). Importantly, SNs displayed glutamate release in response to KCl but not NaCl ruling out an osmotic-mediated effect (Fig. 2D). The $CaCl_2$/KCl effect was blocked by $CdCl_2$, a voltage-gated Ca^{2+} channel blocker, producing values similar to that of EGTA (Fig. 2D). Thus for all subsequent experiments, the minimal value for SN glutamate release was set as the basal value due to simple additions of either H_2O or EGTA alone.

SN additions alone did not alter glutamate standard curves (Fig. 2C). Approximately, 50% of SN stimulated (Ca^{2+}/K^{+}) glutamate release was lost after 24 hour storage at 4°C, while freeze-thawing of SNs resulted in complete loss of stimulated release accompanied by high levels of basal glutamate release (unpublished data). The glutamate transporter inhibitor TBOA (100 μM)(Shimamoto et al., 1998) also increased SN glutamate levels, indicating

transporter activity consistent with tripartite synapses (pre/post synaptic, astrocytic)(Perea et al., 2009)(Fig. 2D; also see Fig. 9).

SN Glutamate Release as a Function of Mouse α-Synuclein Genotype

To extend our previous neurophysiological observations of preynaptic glutamate release in α-synuclein mouse models (Watson et al., 2009), the Amplex Red/glutamate oxidase-based assay was used initially to compare glutamate release in SNs from control WT mice expressing endogenous mouse, α-synuclein ASOTg mice overexpressing human α-synuclein (~23 fold > endogenous WT levels), and KO mice not expressing α-synuclein (Fig. 3). Data, normalized to % of an averaged basal value obtained for all WT mice, showed that glutamate release (both basal and stimulated) was higher in ASOTg SNs but lower in KO SNs relative to WT controls ($P<0.05$, Two Way ANOVA, for pairwise comparisons). Overall the genotype comparisons suggest a dependence of Ca^{2+}/K^{+}-stimulated glutamate release dependent on α-synuclein concentrations.

SN Glutamate Release in Response to Aggregated α-Synuclein

Fibrillation of α-Synuclein—Since mounting evidence indicates that aggregated forms of α-synuclein, principally fibrils and soluble oligomers, are primarily responsible for much of the pathology underlying PD (Roberts and Brown, 2015; Villar-Pique et al., 2015), it was important to examine the role of aggregated α-synuclein proteoforms in modulating presynaptic functions along with monomeric forms. A variety of approaches were used to generate multiple forms of fibrillated α-synuclein (Fig. 4). Initially, recombinant monomers of native, full-length α-synuclein were aggregated by shaking in the presence of 100 mM GdnCl. This method resulted in a typical fluorescence curve characterized by lag, exponential, and stationary phases using TFT as the probe for amyloid structures enriched in β-sheet (Fig. 4A)(Ban et al., 2003; Chattopadhyay et al., 2008; Cohen et al., 2012). It was important to examine also the acetylated form, since it represents a major posttranslational modification in human brain (Fauvet et al., 2013; Sarafian et al., 2013). The NH_2-terminally acetylated form of α-synuclein displayed a similar TFT time course of fluorescence for fibrillation, but often with much lower final stationary levels relative to the native form (unpublished data)(also see Fauvet et al., 2013). Thus the native, non-acetylated form was used in subsequent fibrillation experiments (see Figs. 5, 6 below).

Control proteins such as histone and IgG as well as monomeric α-synuclein displayed little or no TFT fluorescence, consistent with lack of amyloid-related aggregation. Surprisingly, fluorescence intensities varied for GdnCl-derived relative to NaCl-derived fibrillations when monitored over time (0–72 hrs). Although similar TFT fluorescence patterns were observed after 40 hours for each salt, fluorescence intensity was elevated in the presence of NaCl relative to GdnCl (Fig. 4B, top right panel). Relative fluorescence intensities also varied when using DCVJ or ANS as probes, which have been reported to preferentially detect oligomeric amyloid structures (Bolognesi et al., 2010; Paslawski et al., 2014). In contrast to TFT results, both DCVJ and ANS fluorescence were higher in the presence of GdnCl relative to NaCl (Fig. 4B, bottom panels), suggesting that there may be elevated amounts of α-synuclein oligomers in the GdnCl-treated fractions.

As shown in Figure 4C, likely fibrils were detected as large molecular weight aggregates between 24 and 72 hours based on their inability to penetrate native-PAGE gels (5%) and their retention in wells. Large molecular weight smears found at earlier time points (0–24 hours) might correspond to pre-fibrillary forms (protofibrils or possibly large oligomeric structures), but would also suggest some of the protein in the monomeric fraction is already aggregated, even at early time points after preparation. Consistent with this notion, a low level of aggregates was observed in some starting monomer fractions examined with TEM (Fig. 4D). Both monomeric and pre-fibrillary forms decreased substantially over time and were for the most part lost at the 72 hour time point. TEM also detected NaCl-derived (Fig. 4E) and GdnCl-derived (Fig. 4F) fibrils along with globular structures possibly corresponding to oligomers at the 72 hour time point in the absence of fluorescent probes. As expected, additional TEM revealed similar populations of fibrils and likely oligomers when monitored with either fluorescent probes TFT, DCV, or ANS (Fig. 4G–I).

Exogenous Fibrillated α-Synuclein Enhanced SN Glutamate Release—In light of evidence for enhanced neurotoxicity with aggregated forms, glutamate release experiments were performed in which either monomeric or fibrillated α-synuclein were added exogenously to WT SNs after final preparation (SN Treated). As shown in Figure 5, the stimulated component (i.e. Ca^{2+}/KCl) of glutamate release (pmol SN glutamate per μg protein) was enhanced when fibrillated forms were added exogenously ($P<0.05$, TwoWay ANOVA, post-hoc comparisons for both fibril vs histone and fibril vs monomer). Exogenous native monomers also appeared to increase glutamate release but were not significantly different than control ($P>0.05$). Similar results were obtained with the acetylated monomeric form (data not shown).

Pre-Incubation of Both Fibrillated and Monomeric α-Synuclein Enhanced SN Glutamate Release—The previous experiments utilizing exogenous applications of α-synuclein suggested the hypothesis that fibrillated forms were more toxic to glutamate release due in part to their preferential uptake and internalization in SN re-vesicularized membranous structures relative to the monomeric forms. To test this hypothesis further, purified proteins were instead pre-incubated with brain tissues during the initial homogenization step for making SNs (Brain Pre-treated, Fig. 6) to facilitate uptake. As expected from the exogenous studies, fibrillated forms of α-synuclein increased the stimulated component of glutamate release from SNs prepared from pre-treated WT forebrain relative to a histone control. The NaCl- and GdnCl + TFT-derived fibrils together with the NH_2-terminally acetylated, monomeric form were significantly different based on post-hoc pairwise comparisons ($P<0.05$, One Way ANOVA). The GdnCl-derived fibrils and native monomer were also significantly different when compared individually with the histone control alone ($P<0.05$, Student paired *t*-test). Moreover in a separate set of experiments, the native monomeric form also enhanced the stimulated component (histone 4.09±0.393, non-acetylated α-Syn 6.81±0.67, N=5 mice)($P<0.05$).

Protease-Resistance of Monomeric α-Synuclein Pre-Incubated with SNs

To verify that brain pre-treatment facilitated internalization of α-synuclein into SNs, monomeric proteins were either added exogenously after the final SN fraction (SN Treated)

or added to the initial homogenization prior to SN fractionation (Brain Pre-treated) to maximize internalization. SNs were then untreated or treated with trypsin and resolved by Western immunoblotting (Fig. 7). The α-synuclein protein alone served as a positive control for maximal trypsin digestion. The use of SNs prepared from KO mice (control lanes) eliminated interference from endogenous mouse synuclein.

After trypsin digestion, the Western immunoblotting analysis revealed that the α-synuclein contained in the Brain Pre-treated SN (middle panel) was resolved as mostly a single band of 15–16 kDa (right panel) similar in size to the untreated full-length monomer (left panel). Conversely, the SN Treated sample showed two bands of roughly equal intensity (top right panel) smaller than the monomer, corresponding to the major protease cleavage products predicted from bottom-up mass spectrometry peptide analysis (see Sarafian et al., 2013). As expected, the α-synuclein protein alone was resolved mostly as the smaller single band of much reduced intensity after tryspin digestion (bottom panels). While immunoblotting assays were not informative for the truncated α-synuclein (aa 1–95) form, SYPRO®Ruby staining did detect trypsin resistance when Brain Pre-treated (data not shown). Overall the data were consistent with internalization of the α-synuclein protein when added prior to homogenization step for SN fractionation, resulting in resistance to protease digestion.

Synaptic Association of Exogenous α-Synuclein Revealed by Immuno-gold/TEM

The trypsin-insensitivity blotting results (Fig. 7) suggested that some of the pre-treated α-synuclein was sequestered and inaccessible to the added trypsin, consistent with incorporation into re-sealed vesicular structures. Internalization could in principle occur in multiple SN membranous structures including both neuronal pre-synaptic and post-synaptic entities along with glial astrocytic endings characteristic of tripartite synapses (Johnson et al., 1997; Perea et al., 2009).

The idea that α-synuclein was internalized in synaptic endings was tested further by immuno-gold/TEM on fixed SN fractions from KO mice treated with α-synuclein antibody (Fig. 8). After pre-incubation with the starting brain tissue prior to SN fractionation, gold labeling was detected associated with synaptic terminals for both fibrillated and monomeric forms (Fig. 8A/B, Brain Pre-treated). In regards to fibrillated forms, it is not clear if this is derived from fibrils or another proteoform such as dissociated monomers or perhaps oligomers. Clusters of intact fibrils were also found extrasynaptically (Fig. 8A).

Enhanced glutamate release in mature SNs treated exogenously with aggregated forms of α-synuclein (Fig. 5) suggested that this was also due to their association with SN membranes and possible internalization. To test this proposal further, the localization of α-synuclein proteoforms, added exogenously to SN preparations from KO mice, was examined in additional immuno-gold/TEM experiments (Fig. 8C/D, SN Treated). Gold labeling was found within multiple synaptic terminals (Fig. 8C), but again it is not clear if this is derived from fibrils or dissociated monomers or oligomers. Exogenously added fibrils were also found in large membranous structures and as extrasynaptic clusters similar to Fig. 8A (data not shown). Gold-labeled monomeric α-synuclein was mostly found extrasynaptically (Fig. 8D). In control experiments, low levels of gold labeled endogenous mouse protein were observed in WT SNs (Fig. 8E), while no gold labeling was evident in KO SNs (Fig. 8F).

Potential Mechanisms Underlying SN Glutamate Release by α-Synuclein: Transporter Inhibition and Membrane Permeabilization?—As reported above, SN glutamate release was increased by exogenous amounts of fibrillated α-synuclein relative to monomeric forms and histone controls. Since TBOA (100 μM), a potent inhibitor of multiple classes of glutamate transporters (neuronal, astrocytic)(Shimamoto et al., 1998), can also enhance glutamate release (see Fig. 2D), together these results raised possibility that glutamate transporter proteins located ubiquitously on pre-/post-synaptic terminals and astrocytic endings are potential membrane targets for fibrillated α-synuclein. When SNs were treated with both TBOA and fibrillated α-synuclein, effects on basal glutamate values were additive suggesting that these agents acted at different sites (Fig. 9A)($P<0.05$, One Way ANOVA, post-hoc *t*-tests for all comparisons except fibrils vs. control and TBOA vs. fibrils). Although stimulated glutamate values from TBOA plus fibrillated α-synuclein treatment also showed an upward trend, they were not completely additive (Fig. 9B). This result was possibly due to depletion of overall SN glutamate stores in response to both depolarization and transporter blockage over the 30 minute time period for the assay.

A second obvious target for exogenous α-synuclein is the presynaptic membrane itself, since numerous reports indicate that aggregated α-synuclein (fibrils, oligomers) relative to the monomeric form preferentially permeabilized neuronal membranes (Lorenzen et al., 2014; Mahul-Mellier et al., 2015; Peelaerts et al., 2015). To test this possibility, a calcein release assay was employed using WT SNs pre-loaded with calcein-AM. At concentrations shown to enhance glutamate release (see Fig. 5, 6), fibrillated α-synuclein failed to stimulate calcein release when added to SNs (Fig. 9C). As a positive control, digitonin induced a large significant increase in calcein release ($P<0.05$ for digitonin vs. control), due to its known ability to create holes in membranes (Schulz, 1990).

Once internalized, one possible presynaptic target site of fibrillated or monomeric α-synuclein, which could explain their effects on SN glutamate release, is VAMP2/synaptobrevin of the SNARE complex (Burre et al., 2010). To test this hypothesis, truncated (1–95aa) α-synuclein, lacking the carboxyl terminal domain that interacts with synaptobrevin (Burre et al., 2012), was added prior to WT brain tissue homogenization to examine SN glutamate release (Fig. 9D). Neither the non-acetylated nor the NH_2-terminally-acetylated truncated forms enhanced glutamate release above that of the histone control ($P>0.05$, One Way ANOVA), consistent with the need for some interaction with the SNARE complex.

DISCUSSION

Utility of the SN Glutamate Assay

Neurochemical assays of glutamate release from synaptic terminals are very much desired to complement more commonly used electrophysiological approaches. There is an added advantage in the ability to measure quantitatively amounts of glutamate under both basal and stimulated release and in response to a variety of pharmacological, genotypic and proteomic conditions. Here a rapid, scaled down method for SN fractionation was combined with Amplex Red fluorescence/glutamate oxidase enzymatic activity to measure synaptic release of glutamate. An enriched population of presynaptic terminals was sampled in SNs freshly

prepared from mouse forebrain to preserve membrane and vesicle integrity. A basal form of glutamate release from SNs was demonstrated that likely reflects the dynamic process of spontaneous miniature events normally recorded with electrophysiological measurements. In addition, a stimulated form of SN release was also detected as Ca^{2+}/K^{+} depolarization-dependent vesicular release from presynaptic terminals based on the appropriate controls (e.g. KCl vs. NaCl, $CaCl_2$ vs. $CdCl_2$, TBOA).

Concentration Dependence of Monomeric α-Synuclein for SN Glutamate Release

Previously, ASOTg mice overexpressing human α-synuclein did not display detectable fibril or oligomer formation (Sarafian et al., 2013), but appeared to have diminished glutamate release relative to WT controls based on measurements of presynaptic forms of synaptic plasticity (Watson et al., 2009). This observation was consistent with other reports suggesting that an excess amount of monomeric α-synuclein was toxic and diminished neurotransmitter release (Cabin et al., 2002; Larsen et al., 2006; Nemani et al., 2010). In contrast, additional reports argued the opposite effect, pointing to enhanced presynaptic modulation by excess monomeric α-synuclein (Liu et al., 2004; Gureviciene et al., 2007; Ronzitti et al., 2014).

To address this question further, neurochemical measurements of presynaptic glutamate release were performed in the present study using a fluorescence-based glutamate assay. SN glutamate levels were compared both between α-synuclein genotypes (WT, ASOTg, KO) and between monomeric and aggregated proteoforms pre-incorporated in SNs and compared side by side. When there was no α-synuclein in the SN terminals (KOs), relative glutamate release was depressed, while additional amounts (over 20-fold higher than endogenous mouse levels) in ASOTg mice (Watson et al., 2009) or pre-internalized in SNs as recombinant full-length monomeric protein instead elevated glutamate levels. Importantly, Western immunoblotting data showed that SN fractions prepared from pre-treated forebrains contained membrane-internalized full-length α-synuclein monomers, based on resistance to protease digestion. Immuno-gold TEM confirmed labeling of α-synuclein monomers in synaptic terminals of SN fractions prepared from pre-treated forebrain.

Thus, these results are more in agreement with positive effect of α-synuclein on neurotransmitter release. Discrepancy between some of the previous neurophysiological studies and the current neurochemical measurements can be explained by different time scales for each assay. For example, electrophysiological measurements record extremely rapid, short-term events at the millisecond level for neurotransmitter release. On the other hand, the neurochemical assay described here measured synaptic events over a much longer timescale of 30 minutes, likely reflecting a steady-state level of both tonic basal, spontaneous release and intermittent Ca^{2+}/K^{+} depolarization-dependent stimulated release from a diversity of synaptic vesicles (Crawford and Kavalali, 2015). It is also conceivable that α-synuclein has differential effects on either basal or stimulated release and this requires different amounts of protein. Nevertheless the assay has provided another set of quantitative tools to accurately measure synaptic glutamate release as a response to a variety of α-synuclein forms and concentrations.

Overall, glutamate measurements for both SN endogenous genotypes (WT, ASOTg, KO) and SNs reconstituted with purified α-synuclein proteoforms pointed to a concentration dependence of α-synuclein on activity-dependent presynaptic glutamate release from forebrain terminals. This proposal is in line with previous reports that α-synuclein performs a chaperone role for SNARE function in presynaptic terminals by directly interacting with synaptobrevin (Burre et al., 2010). To test if this mechanism was involved in monomeric α-synuclein's effect on glutamate release, a truncated form of α-synuclein lacking carboxyl terminal residues 96–140 was prepared and pre-incorporated into SNs. The truncated form failed to stimulate glutamate release above control levels, consistent with a role for α-synuclein/SNARE interactions. However, other presynaptic targets such as Rab proteins and mitochondrial membrane proteins cannot be ruled out (Wislet-Gendebien et al., 2006; Gitler et al., 2008; Nakamura et al., 2008).

Aggregated Forms of α-Synuclein Enhanced SN Glutamate Release

The unique ability of fibrillated forms of α-synuclein to stimulate glutamate release after brief acute (30 minutes) exogenous exposure to mature SN preparations was consistent with reports that fibrillated α-synuclein has greater membrane permeating ability and greater toxicity than monomeric forms (Desplats et al., 2009; Varkey et al., 2010; Chaudhary et al., 2014; Lorenzen et al., 2014; Pacheco et al., 2015). In the present study, evidence for fibril association with membranes and internalization was based mainly on immuno-gold TEM analyses of SN fractions. While the TEM has the limitation of not being inherently quantitative, on a qualitative level the TEM micrographs clearly revealed intact fibril association with a variety of SN membranous structures. Indeed, immuno-gold TEM revealed that, along with extrasynaptic clustering of fibrils near membranes, labeling was associated with synaptic terminals of SNs treated exogenously with fibrillated α-synuclein. Whether fibrillated forms, once inside synaptic terminals, can bind directly to and modulate synaptic vesicles is unknown. Since the non-amyloid component (NAC) hydrophobic core region (61–95) is most prone to contribute to β-sheet enriched amyloid structures of α-synuclein (Burre et al., 2012), both NH_2-and COOH-terminal regions of internalized fibrils and/or oligomers may remain exposed (Murray et al., 2003) and potentially interact with the same presynaptic targets as monomers. It is also possible that by binding to synaptic membranes or once inside such structures, fibrillated α-synuclein can facilitate monomer uptake and/or dissociate, releasing locally high concentrations of monomeric and/or oligomeric α-synuclein (Volpicelli-Daley et al., 2011; Cremades et al., 2012; Mahul-Mellier et al., 2015). Membrane interaction by a subpopulation of α-helical tetrameric forms of α-synuclein also cannot be ruled out (Bartels et al., 2011; Wang et al., 2011). It is likely that for exogenous application, α-synuclein fibrils are the main active forms involved in membrane uptake. Monomer fractions alone (possibly containing a subpopulation of oligomers) did not significantly enhance glutamate release.

It should be noted that most of the aggregated α-synuclein samples used for the SN glutamate assays were obtained at later phases of fibrillation (24–72 hrs) when a wide spectrum of amyloid structures (oligomers, protofibrils, mature fibrils) were expected. Combined immunoblotting and TEM confirmed a heterogeneous population of fibrils but oligomer formation likely varied for each preparation. Use of different fluorescent probes

and GdnCl to select for oligomers appeared quite promising but could not be used in SN glutamate measurements because of their interference with the assay. Enrichment for soluble oligomeric and fibril forms by micro-centrifugation revealed no detectable difference in evoked glutamate release when comparing oligomer-enriched and fibril-enriched samples (personal observations). It is possible that extensive interconversion of aggregated forms occurred following exposure to SNs or that the total α-synuclein monomeric amount and not the structural form was most important for the magnitude of glutamate release. It will be critically important to have an enriched homogenous population (in progress) of oligomeric forms to test in future experiments.

Interestingly, both GdnCl and TFT, when added alone, increased SN-glutamate release (unpublished data) raising the possibility of their direct effects on SN glutamate release independent of α-synuclein proteoforms. It has been reported previously that GdnCl can have spurious effects on synaptic function (Banks, 1978), but TFT's effects were to our knowledge not reported previously. It is conceivable that the high levels of glutamate release caused by pre-incorporation of α-synuclein were, in part, caused by the presence of fibril-associated TFT. However, TFT was also observed to greatly enhance α-synuclein fibrillation based on ~2-fold greater pellet sizes following 12,000 × *g* centrifugation (unpublished data) and this may have contributed to glutamate release. This finding is consistent with a literature report describing accelerated α-synuclein fibrillation caused by TFT (Coelho-Cerqueira et al., 2014). An alternative explanation is that TFT stabilizes fibrillar α-synuclein conformations when it binds to β-sheet-enriched amyloid structures (Landau et al., 2011).

Mechanism for Enhanced Glutamate Release from SNs Incubated with Exogenous Aggregated α-Synuclein?

There are multiple scenarios that can explain how exogenous applications of fibrillated α-synuclein can alter glutamate levels released from SNs. One potential mechanism is inhibition of glutamate re-uptake by one or more tripartite synaptic transporters localized on presynaptic, postsynaptic and astrocytic endings (Divito and Underhill, 2014). Since broad-range transporter inhibition by TBOA greatly increased basal glutamate release, it was clear that transporter-reuptake (likely both neuronal and astrocytic) systems were functional in each SN fraction. Inhibition of one or more of these re-uptake systems by fibrillated α-synuclein would elevate levels of external glutamate. However, since the degree of fibrillated α-synuclein-induced glutamate release was substantially increased when TBOA were added, transporter function was considered unlikely to contribute to fibrillated α-synuclein's actions. In other words TBOA and fibrillated α-synuclein appeared to act additively and thus independently.

An additional mechanism could be membrane permeabilization. Numerous reports suggested that fibrillated/oligomeric α-synuclein can penetrate and permeabilize lipid membranes including neuronal membranes (Tsigelny et al., 2012; Chaudhary et al., 2014; Lorenzen et al., 2014; Pacheco et al., 2015). Since physical disruption of synaptic vesicles on the presynaptic membrane would likely result in enhanced SN glutamate release, the effect of fibrillated α-synuclein on SN membrane permeabilization was investigated using SNs pre-loaded with calcein-AM. Fibrillated α-synuclein at concentrations (~ 0.7 μM)

shown previously to enhance SN-glutamate release failed to promote calcein release suggesting that SN membrane permeabilization does not account for elevated glutamate release. It should be noted that previous permeabilization assays used much higher concentrations (as much as 5–10 fold higher) of α-synuclein proteoforms than those used here, so membrane disruption cannot be ruled out with higher amounts of fibrillated α-synuclein. Other potential plasma membrane targets for aggregated α-synuclein include presynaptic Cav2.2 channels (Ronzitti et al., 2014), the Na^+/K^+ ATPase pump (Shrivastava et al., 2015), and depolarization-dependent release of glutamate from astrocytic endings contained in SN fractions (Navarrete et al., 2013).

To summarize, *first* an enzyme-based assay was implemented that can rapidly measure quantitative amounts of basal and stimulated (K^+/Ca^{2+} depolarization) glutamate released from biochemically prepared synaptic endings contained in SN fractions. This assay has broad utility for studying synaptic mechanisms and the effects of a wide variety of proteins delivered either internally or exogenously. *Second*, although our previous neurophysiological studies (Watson et al., 2009) as well as others (reviewed in Bendor et al., 2013) were consistent with alterations in presynaptic glutamate release in the face of the central PD-related protein α-synuclein, the present study to our knowledge is the first to measure neurochemically increased synaptic glutamate in direct response to various amounts and aggregated proteoforms of human α-synuclein. Enhanced amounts of glutamate release from SN fractions were found in response to pre-incorporation of excess amounts of both monomeric and fibrillated forms of α-synuclein. Moreover, after brief exogenous applications of fibrillated forms of α-synuclein, the protein was found closely associated with SN membranous structures and enhanced synaptic glutamate release, consistent with partial uptake by synaptic terminals. These studies lend support to the concept that excitotoxicity (Ambrosi et al., 2014) due to enhanced glutamate release, by either overexpressed monomeric or extrasynaptic aggregated α-synuclein, should be considered as a potential neuropathological pathway during the progression of PD and other synucleinopathies.

Acknowledgments

FUNDING: Julian Whitelegge was supported by the UCSD/UCLA Diabetes Research Center (P30 DK063491). UCLA-DOE Protein Expression Technology Center was supported by the U.S. Department of Energy, Office of Biological and Environmental Research (BER) program under Award Number DE-FC02-02ER63421.

Thanks to Mark Arbing for recombinant proteins which were prepared by the UCLA-DOE Protein Expression Technology Center Mice [supported by the U.S. Department of Energy, Office of Biological and Environmental Research (BER) program under Award Number DE-FC02-02ER63421]. Ralph Langen at the University of Southern California graciously provided the pRK172 plasmid for recombinant human α-synuclein. Special thanks to Asa Hatami for advice on amyloid structures and Anna Caputo and Felix Schweizer for advice on the SN glutamate assay. Many thanks to the UCLA labs of Michael Levine (especially Jan Asai) and Marie-Francoise Chesselet, and also Eliezer Masliah at UCSD for providing α-synuclein mouse models. Donna Crandall deserves additional gratitude for art work and illustrations. The authors are grateful to undergraduates Anastasia Kunz, Grigor Serobyan, and Amneh Yacoub for laboratory research assistance. Lastly thanks to Carlos Cepeda, Josh Barry, and Sandra Holley for insightful advice and feedback on the manuscript and overall project.

LITERATURE CITED

Ambrosi G, Cerri S, Blandini F. A further update on the role of excitotoxicity in the pathogenesis of Parkinson's disease. J Neural Transm (Vienna). 2014; 121:849–859. [PubMed: 24380931]

Ban T, Hamada D, Hasegawa K, Naiki H, Goto Y. Direct observation of amyloid fibril growth monitored by thioflavin T fluorescence. J Biol Chem. 2003; 278:16462–16465. [PubMed: 12646572]

Banks FW. The effect of guanidine on transmitter release in the ciliary ganglion of the chick. J Physiol. 1978; 278:425–433. [PubMed: 209168]

Bartels T, Choi JG, Selkoe DJ. alpha-Synuclein occurs physiologically as a helically folded tetramer that resists aggregation. Nature. 2011; 477:107–110. [PubMed: 21841800]

Bendor JT, Logan TP, Edwards RH. The function of alpha-synuclein. Neuron. 2013; 79:1044–1066. [PubMed: 24050397]

Bolognesi B, Kumita JR, Barros TP, Esbjorner EK, Luheshi LM, Crowther DC, Wilson MR, Dobson CM, Favrin G, Yerbury JJ. ANS binding reveals common features of cytotoxic amyloid species. ACS Chem Biol. 2010; 5:735–740. [PubMed: 20550130]

Burre J, Sharma M, Sudhof TC. Systematic mutagenesis of alpha-synuclein reveals distinct sequence requirements for physiological and pathological activities. J Neurosci. 2012; 32:15227–15242. [PubMed: 23100443]

Burre J, Sharma M, Sudhof TC. Definition of a molecular pathway mediating alpha-synuclein neurotoxicity. J Neurosci. 2015; 35:5221–5232. [PubMed: 25834048]

Burre J, Sharma M, Tsetsenis T, Buchman V, Etherton MR, Sudhof TC. Alpha-synuclein promotes SNARE-complex assembly in vivo and in vitro. Science. 2010; 329:1663–1667. [PubMed: 20798282]

Cabin DE, Shimazu K, Murphy D, Cole NB, Gottschalk W, McIlwain KL, Orrison B, Chen A, Ellis CE, Paylor R, Lu B, Nussbaum RL. Synaptic vesicle depletion correlates with attenuated synaptic responses to prolonged repetitive stimulation in mice lacking alpha-synuclein. J Neurosci. 2002; 22:8797–8807. [PubMed: 12388586]

Chang JW, Arnold MM, Rozenbaum A, Caputo A, Schweizer FE, Huynh M, Mathern GW, Sarafian TA, Watson JB. Synaptoneurosome micromethod for fractionation of mouse and human brain, and primary neuronal cultures. J Neurosci Methods. 2012; 211:289–295. [PubMed: 23017979]

Chattopadhyay M, Durazo A, Sohn SH, Strong CD, Gralla EB, Whitelegge JP, Valentine JS. Initiation and elongation in fibrillation of ALS-linked superoxide dismutase. Proc Natl Acad Sci U S A. 2008; 105:18663–18668. [PubMed: 19022905]

Chaudhary H, Stefanovic AN, Subramaniam V, Claessens MM. Membrane interactions and fibrillization of alpha-synuclein play an essential role in membrane disruption. FEBS Lett. 2014; 588:4457–44563. [PubMed: 25448986]

Chen SW, Drakulic S, Deas E, Ouberai M, Aprile FA, Arranz R, Ness S, Roodveldt C, Guilliams T, De-Genst EJ, Klenerman D, Wood NW, Knowles TP, Alfonso C, Rivas G, Abramov Y, Valpuesta JM, Dobson CM, Cremades N. Structural characterization of toxic oligomers that are kinetically trapped during alpha-synuclein fibril formation. Proc Natl Acad Sci U S A. 2015; 112:E1994–E2003. [PubMed: 25855634]

Choi BK, Choi MG, Kim JY, Yang Y, Lai Y, Kweon DH, Lee NK, Shin YK. Large alpha-synuclein oligomers inhibit neuronal SNARE-mediated vesicle docking. Proc Natl Acad Sci U S A. 2013; 110:4087–4092. [PubMed: 23431141]

Coelho-Cerqueira E, Pinheiro AS, Follmer C. Pitfalls associated with the use of Thioflavin-T to monitor anti-fibrillogenic activity. Bioorg Med Chem Lett. 2014; 24:3194–3198. [PubMed: 24835632]

Cohen SI, Vendruscolo M, Dobson CM, Knowles TP. From macroscopic measurements to microscopic mechanisms of protein aggregation. J Mol Biol. 2012; 421:160–171. [PubMed: 22406275]

Crawford DC, Kavalali ET. Molecular underpinnings of synaptic vesicle pool heterogeneity. Traffic. 2015; 16:338–364. [PubMed: 25620674]

Cremades N, Cohen SI, Deas E, Abramov AY, Chen AY, Orte A, Sandal M, Clarke RW, Dunne P, Aprile FA, Bertoncini CW, Wood NW, Knowles TP, Dobson CM, Klenerman D. Direct observation of the interconversion of normal and toxic forms of alpha-synuclein. Cell. 2012; 149:1048–1059. [PubMed: 22632969]

Danzer KM, Haasen D, Karow AR, Moussaud S, Habeck M, Giese A, Kretzschmar H, Hengerer B, Kostka M. Different species of alpha-synuclein oligomers induce calcium influx and seeding. J Neurosci. 2007; 27:9220–9232. [PubMed: 17715357]

Dauer W, Przedborski S. Parkinson's disease: mechanisms and models. Neuron. 2003; 39:889–909. [PubMed: 12971891]

Der-Sarkissian A, Jao CC, Chen J, Langen R. Structural organization of alpha-synuclein fibrils studied by site-directed spin labeling. J Biol Chem. 2003; 278:37530–37535. [PubMed: 12815044]

Desplats P, Lee HJ, Bae EJ, Patrick C, Rockenstein E, Crews L, Spencer B, Masliah E, Lee SJ. Inclusion formation and neuronal cell death through neuron-to-neuron transmission of alpha-synuclein. Proc Natl Acad Sci U S A. 2009; 106:13010–13015. [PubMed: 19651612]

Dettmer U, Newman AJ, von Saucken VE, Bartels T, Selkoe D. KTKEGV repeat motifs are key mediators of normal alpha-synuclein tetramerization: Their mutation causes excess monomers and neurotoxicity. Proc Natl Acad Sci U S A. 2015; 112:9596–9601. [PubMed: 26153422]

DeWitt DC, Rhoades E. alpha-Synuclein can inhibit SNARE-mediated vesicle fusion through direct interactions with lipid bilayers. Biochemistry. 2013; 52:2385–2387. [PubMed: 23528131]

Diao J, Burre J, Vivona S, Cipriano DJ, Sharma M, Kyoung M, Sudhof TC, Brunger AT. Native alpha-synuclein induces clustering of synaptic-vesicle mimics via binding to phospholipids and synaptobrevin-2/VAMP2. eLife. 2013; 2:e00592. [PubMed: 23638301]

Divito CB, Underhill SM. Excitatory amino acid transporters: roles in glutamatergic neurotransmission. Neurochem Int. 2014; 73:172–180. [PubMed: 24418112]

Fauvet B, Butterfield SM, Fuks J, Brik A, Lashuel HA. One-pot total chemical synthesis of human alpha-synuclein. Chem Commun. 2013; 49:9254–9256.

Fauvet B, Fares MB, Samuel F, Dikiy I, Tandon A, Eliezer D, Lashuel HA. Characterization of semisynthetic and naturally Nalpha-acetylated alpha-synuclein in vitro and in intact cells: implications for aggregation and cellular properties of alpha-synuclein. J Biol Chem. 2012; 287:28243–28262. [PubMed: 22718772]

Fleming SM, Tetreault NA, Mulligan CK, Hutson CB, Masliah E, Chesselet MF. Olfactory deficits in mice overexpressing human wildtype alpha-synuclein. Eur J Neurosci. 2008; 28:247–256. [PubMed: 18702696]

Gitler AD, Bevis BJ, Shorter J, Strathearn KE, Hamamichi S, Su LJ, Caldwell KA, Caldwell GA, Rochet JC, McCaffery JM, Barlowe C, Lindquist S. The Parkinson's disease protein alpha-synuclein disrupts cellular Rab homeostasis. Proc Natl Acad Sci U S A. 2008; 105:145–150. [PubMed: 18162536]

Gureviciene I, Gurevicius K, Tanila H. Role of alpha-synuclein in synaptic glutamate release. Neurobiol Dis. 2007; 28:83–89. [PubMed: 17689254]

Houlden H, Singleton AB. The genetics and neuropathology of Parkinson's disease. Acta Neuropathol. 2012; 124:325–338. [PubMed: 22806825]

Johnson M, Coulton AT, Geeves MA, Mulvihill DP. Targeted amino-terminal acetylation of recombinant proteins in E. coli. PLoS One. 2010; 5(12):e15801. [PubMed: 21203426]

Johnson MW, Chotiner JK, Watson JB. Isolation and characterization of synaptoneurosomes from single rat hippocampal slices. J Neurosci Methods. 1997; 77:151–156. [PubMed: 9489891]

Kordower JH, Chu Y, Hauser RA, Freeman TB, Olanow CW. Lewy body-like pathology in long-term embryonic nigral transplants in Parkinson's disease. Nat Med. 2008; 14:504–506. [PubMed: 18391962]

Landau M, Sawaya MR, Faull KF, Laganowsky A, Jiang L, Sievers SA, Liu J, Barrio JR, Eisenberg D. Towards a pharmacophore for amyloid. PLoS Biol. 2011; 9:e1001080. [PubMed: 21695112]

Larsen KE, Schmitz Y, Troyer MD, Mosharov E, Dietrich P, Quazi AZ, Savalle M, Nemani V, Chaudhry FA, Edwards RH, Stefanis L, Sulzer D. Alpha-synuclein overexpression in PC12 and chromaffin cells impairs catecholamine release by interfering with a late step in exocytosis. J Neurosci. 2006; 26:11915–11922. [PubMed: 17108165]

Lasser C, Eldh M, Lotvall J. Isolation and characterization of RNA-containing exosomes. J Vis Exp. 2012; (59):e3037. [PubMed: 22257828]

Li JY, Englund E, Holton JL, Soulet D, Hagell P, Lees AJ, Lashley T, Quinn NP, Rehncrona S, Bjorklund A, Widner H, Revesz T, Lindvall O, Brundin P. Lewy bodies in grafted neurons in

subjects with Parkinson's disease suggest host-to-graft disease propagation. Nat Med. 2008; 14:501–503. [PubMed: 18391963]

Liu S, Ninan I, Antonova I, Battaglia F, Trinchese F, Narasanna A, Kolodilov N, Dauer W, Hawkins RD, Arancio O. alpha-Synuclein produces a long-lasting increase in neurotransmitter release. EMBO J. 2004; 23:4506–4516. [PubMed: 15510220]

Lorenzen N, Nielsen SB, Buell AK, Kaspersen JD, Arosio P, Vad BS, Paslawski W, Christiansen G, Valnickova-Hansen Z, Andreasen M, Enghild JJ, Pedersen JS, Dobson CM, Knowles TP, Otzen DE. The role of stable alpha-synuclein oligomers in the molecular events underlying amyloid formation. J Amer Chem Soc. 2014; 136:3859–3868. [PubMed: 24527756]

Luk KC, Lee VM. Modeling Lewy pathology propagation in Parkinson's disease. Parkinsonism Relat Disord. 2014; 20(Suppl 1):S85–S87. [PubMed: 24262196]

Luth ES, Stavrovskaya IG, Bartels T, Kristal BS, Selkoe DJ. Soluble, prefibrillar alpha-synuclein oligomers promote complex I-dependent, Ca^{2+}-induced mitochondrial dysfunction. J Biol Chem. 2014; 289:21490–21507. [PubMed: 24942732]

Mahul-Mellier AL, Vercruysse F, Maco B, Ait-Bouziad N, De Roo M, Muller D, Lashuel HA. Fibril growth and seeding capacity play key roles in alpha-synuclein-mediated apoptotic cell death. Cell Death Differ. 2015; 22:2107–2122. [PubMed: 26138444]

Martinez Z, Zhu M, Han S, Fink AL. GM1 specifically interacts with alpha-synuclein and inhibits fibrillation. Biochemistry. 2007; 46:1868–1877. [PubMed: 17253773]

Murray IVJ, Giasson BI, Quinn SM, Koppaka V, Axelsen PH, Ischiropoulos H, Trojanowski JQ, Lee VM-Y. Role of α-synuclein carboxy-terminus on fibril formation in vitro. Biochemistry. 2003; 42:8530–8540. [PubMed: 12859200]

Nakamura K, Nemani VM, Wallender EK, Kaehlcke K, Ott M, Edwards RH. Optical reporters for the conformation of alpha-synuclein reveal a specific interaction with mitochondria. J Neurosci. 2008; 28:12305–12317. [PubMed: 19020024]

Navarrete M, Perea G, Maglio L, Pastor J, Garcia de Sola R, Araque A. Astrocyte calcium signal and gliotransmission in human brain tissue. Cereb Cortex. 2013; 23:1240–1246. [PubMed: 22581850]

Nemani VM, Lu W, Berge V, Nakamura K, Onoa B, Lee MK, Chaudhry FA, Nicoll RA, Edwards RH. Increased expression of alpha-synuclein reduces neurotransmitter release by inhibiting synaptic vesicle reclustering after endocytosis. Neuron. 2010; 65:66–79. [PubMed: 20152114]

Osterberg VR, Spinelli KJ, Weston LJ, Luk KC, Woltjer RL, Unni VK. Progressive aggregation of alpha-synuclein and selective degeneration of lewy inclusion-bearing neurons in a mouse model of parkinsonism. Cell Rep. 2015; 10:1252–1260. [PubMed: 25732816]

Pacheco CR, Morales CN, Ramirez AE, Munoz FJ, Gallegos SS, Caviedes PA, Aguayo LG, Opazo CM. Extracellular alpha-synuclein alters synaptic transmission in brain neurons by perforating the neuronal plasma membrane. J Neurochem. 2015; 132:731–741. [PubMed: 25669123]

Paslawski W, Andreasen M, Nielsen SB, Lorenzen N, Thomsen K, Kaspersen JD, Pedersen JS, Otzen DE. High stability and cooperative unfolding of alpha-synuclein oligomers. Biochemistry. 2014; 53:6252–6263. [PubMed: 25216651]

Peelaerts W, Bousset L, Van der Perren A, Moskalyuk A, Pulizzi R, Giugliano M, Van den Haute C, Melki R, Baekelandt V. alpha-Synuclein strains cause distinct synucleinopathies after local and systemic administration. Nature. 2015; 522:340–344. [PubMed: 26061766]

Perea G, Navarrete M, Araque A. Tripartite synapses: astrocytes process and control synaptic information. TINS. 2009; 32:421–431. [PubMed: 19615761]

Prusiner SB, Woerman AL, Mordes DA, Watts JC, Rampersaud R, Berry DB, Patel S, Oehler A, Lowe JK, Kravitz SN, Geschwind DH, Glidden DV, Halliday GM, Middleton LT, Gentleman SM, Grinberg LT, Giles K. Evidence for alpha-synuclein prions causing multiple system atrophy in humans with parkinsonism. Proc Natl Acad Sci U S A. 2015; 112:E5308–E5317. [PubMed: 26324905]

Roberts HL, Brown DR. Seeking a mechanism for the toxicity of oligomeric alpha-synuclein. Biomolecules. 2015; 5:282–305. [PubMed: 25816357]

Rockenstein E, Mallory M, Hashimoto M, Song D, Shults CW, Lang I, Masliah E. Differential neuropathological alterations in transgenic mice expressing alpha-synuclein from the platelet-

derived growth factor and Thy-1 promoters. J Neurosci Res. 2002; 68:568–578. [PubMed: 12111846]

Ronzitti G, Bucci G, Emanuele M, Leo D, Sotnikova TD, Mus LV, Soubrane CH, Dallas ML, Thalhammer A, Cingolani LA, Mochida S, Gainetdinov RR, Stephens GJ, Chieregatti E. Exogenous alpha-synuclein decreases raft partitioning of Cav2.2 channels inducing dopamine release. J Neurosci. 2014; 34:10603–10615. [PubMed: 25100594]

Roychaudhuri R, Yang M, Deshpande A, Cole GM, Frautschy S, Lomakin A, Benedek GB, Teplow DB. C-terminal turn stability determines assembly differences between Abeta40 and Abeta42. J Mol Biol. 2013; 425:292–308. [PubMed: 23154165]

Sarafian TA, Ryan CM, Souda P, Masliah E, Kar UK, Vinters HV, Mathern GW, Faull KF, Whitelegge JP, Watson JB. Impairment of mitochondria in adult mouse brain overexpressing predominantly full-length, N-terminally acetylated human alpha-synuclein. PLoS One. 2013; 8(5):e63557. [PubMed: 23667637]

Schulz I. Permeabilizing cells: some methods and applications for the study of intracellular processes. Method Enzymol. 1990; 192:280–300.

Shimamoto K, Lebrun B, Yasuda-Kamatani Y, Sakaitani M, Shigeri Y, Yumoto N, Nakajima T. DL-threo-beta-benzyloxyaspartate, a potent blocker of excitatory amino acid transporters. Mol Pharmacol. 1998; 53:195–201. [PubMed: 9463476]

Shrivastava AN, Redeker V, Fritz N, Pieri L, Almeida LG, Spolidoro M, Liebmann T, Bousset L, Renner M, Lena C, Aperia A, Melki R, Triller A. alpha-synuclein assemblies sequester neuronal alpha3-Na^+/K^+-ATPase and impair Na^+ gradient. EMBO J. 2015; 34:2408–2423. [PubMed: 26323479]

Shulman JM, De Jager PL, Feany MB. Parkinson's disease: genetics and pathogenesis. Annu Rev Pathol. 2011; 6:193–222. [PubMed: 21034221]

Spinelli KJ, Taylor JK, Osterberg VR, Churchill MJ, Pollock E, Moore C, Meshul CK, Unni VK. Presynaptic alpha-synuclein aggregation in a mouse model of Parkinson's disease. J Neurosci. 2014; 34:2037–2050. [PubMed: 24501346]

Sreekumar PG, Kannan R, Kitamura M, Spee C, Barron E, Ryan SJ, Hinton DR. alphaB crystallin is apically secreted within exosomes by polarized human retinal pigment epithelium and provides neuroprotection to adjacent cells. PLoS One. 2010; 5(10):e12578. [PubMed: 20949024]

Tsang SH, Woodruff ML, Hsu CW, Naumann MC, Cilluffo M, Tosi J, Lin CS. Function of the asparagine 74 residue of the inhibitory gamma-subunit of retinal rod cGMP-phophodiesterase (PDE) in vivo. Cellular Signalling. 2011; 23:1584–1589. [PubMed: 21616145]

Tsigelny IF, Sharikov Y, Wrasidlo W, Gonzalez T, Desplats PA, Crews L, Spencer B, Masliah E. Role of alpha-synuclein penetration into the membrane in the mechanisms of oligomer pore formation. FEBS J. 2012; 279:1000–1013. [PubMed: 22251432]

Valencia A, Sapp E, Kimm JS, McClory H, Ansong KA, Yohrling G, Kwak S, Kegel KB, Green KM, Shaffer SA, Aronin N, DiFiglia M. Striatal synaptosomes from Hdh140Q/140Q knock-in mice have altered protein levels, novel sites of methionine oxidation, and excess glutamate release after stimulation. J Huntingtons Dis. 2013; 2:459–475. [PubMed: 24696705]

Varkey J, Isas JM, Mizuno N, Jensen MB, Bhatia VK, Jao CC, Petrlova J, Voss JC, Stamou DG, Steven AC, Langen R. Membrane curvature induction and tubulation are common features of synucleins and apolipoproteins. J Biol Chem. 2010; 285:32486–32493. [PubMed: 20693280]

Villar-Pique A, da Fonseca TL, Outeiro TF. Structure, function and toxicity of alpha-synuclein: the Bermuda triangle in synucleinopathies. J Neurochem. 2015

Volpicelli-Daley LA, Luk KC, Patel TP, Tanik SA, Riddle DM, Stieber A, Meaney DF, Trojanowski JQ, Lee VM. Exogenous alpha-synuclein fibrils induce Lewy body pathology leading to synaptic dysfunction and neuron death. Neuron. 2011; 72:57–71. [PubMed: 21982369]

Wang W, Perovic I, Chittuluru J, Kaganovich A, Nguyen LT, Liao J, Auclair JR, Johnson D, Landeru A, Simorellis AK, Ju S, Cookson MR, Asturias FJ, Agar JN, Webb BN, Kang C, Ringe D, Petsko GA, Pochapsky TC, Hoang QQ. A soluble alpha-synuclein construct forms a dynamic tetramer. Proc Natl Acad Sci U S A. 2011; 108:17797–17802. [PubMed: 22006323]

Watson JB, Hatami A, David H, Masliah E, Roberts K, Evans CE, Levine MS. Alterations in corticostriatal synaptic plasticity in mice overexpressing human alpha-synuclein. Neuroscience. 2009; 159:501–513. [PubMed: 19361478]

Wislet-Gendebien S, D'Souza C, Kawarai T, St George-Hyslop P, Westaway D, Fraser P, Tandon A. Cytosolic proteins regulate alpha-synuclein dissociation from presynaptic membranes. J Biol Chem. 2006; 28:32148–32155.

SIGIFICANCE STATEMENT

How the α-synuclein protein becomes toxic to neuronal communication in Parkinson's disease remains unclear. The current study showed that aggregated forms of α-synuclein were preferentially taken up by synaptic terminals and abnormally released elevated amounts of the neurotransmitter glutamate.

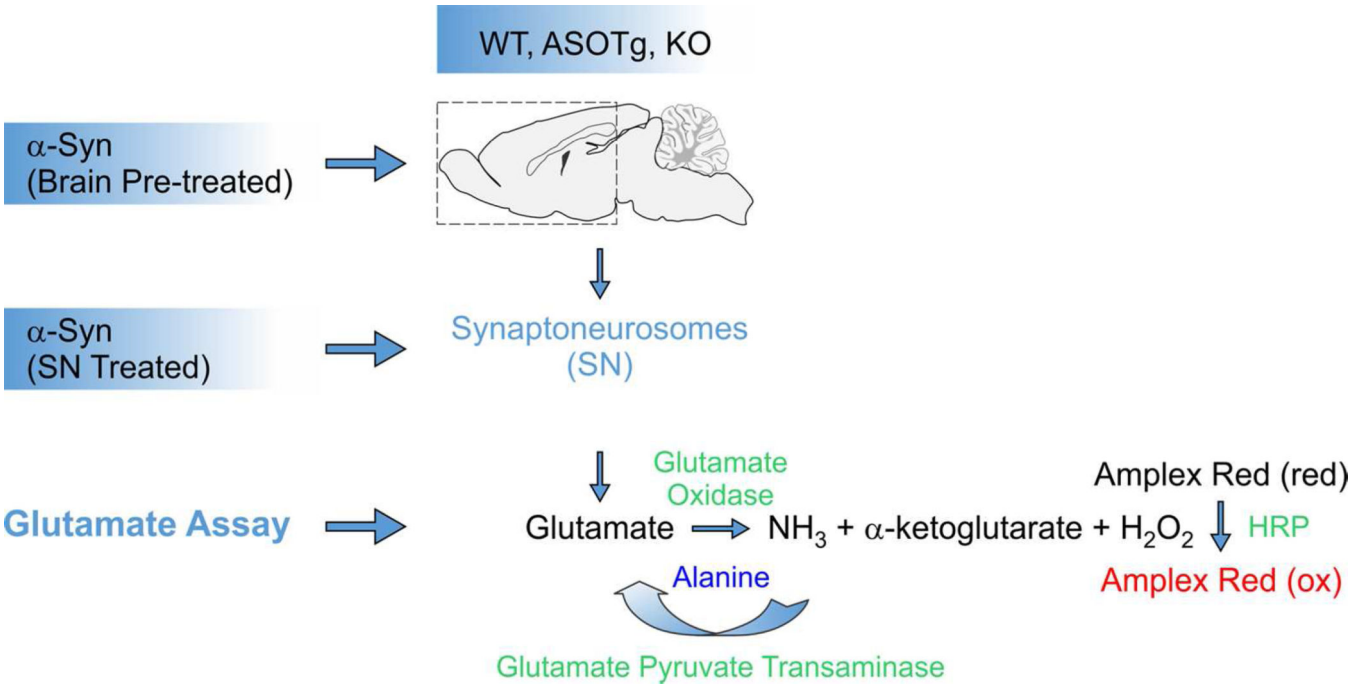

Figure 1. Synaptoneurosomes (SNs) fractionation and glutamate assay

SNs were prepared as described (Chang et al., 2012) from forebrains of different genotypic mice (WT, ASOTg, KO). For reconstitution experiments, recombinant human α-synuclein (α-Syn) proteoforms (monomers, fibrillated) were either pre-incubated with WT brain tissue (Brain Pre-treated) prior to SN fractionation or post-incubated (SN treated) after the final SN preparation. Glutamate oxidase activity coupled to horseradish peroxidase (HRP) mediated Amplex Red fluorescence (Amplex® Red Glutamic Acid/Glutamate Oxidase Assay Kit, ThermoFisher) was used to measure either basal (H_2O ± EGTA) or stimulated (40 mM KCl/0.5 mM $CaCl_2$) glutamate release from isolated SNs.

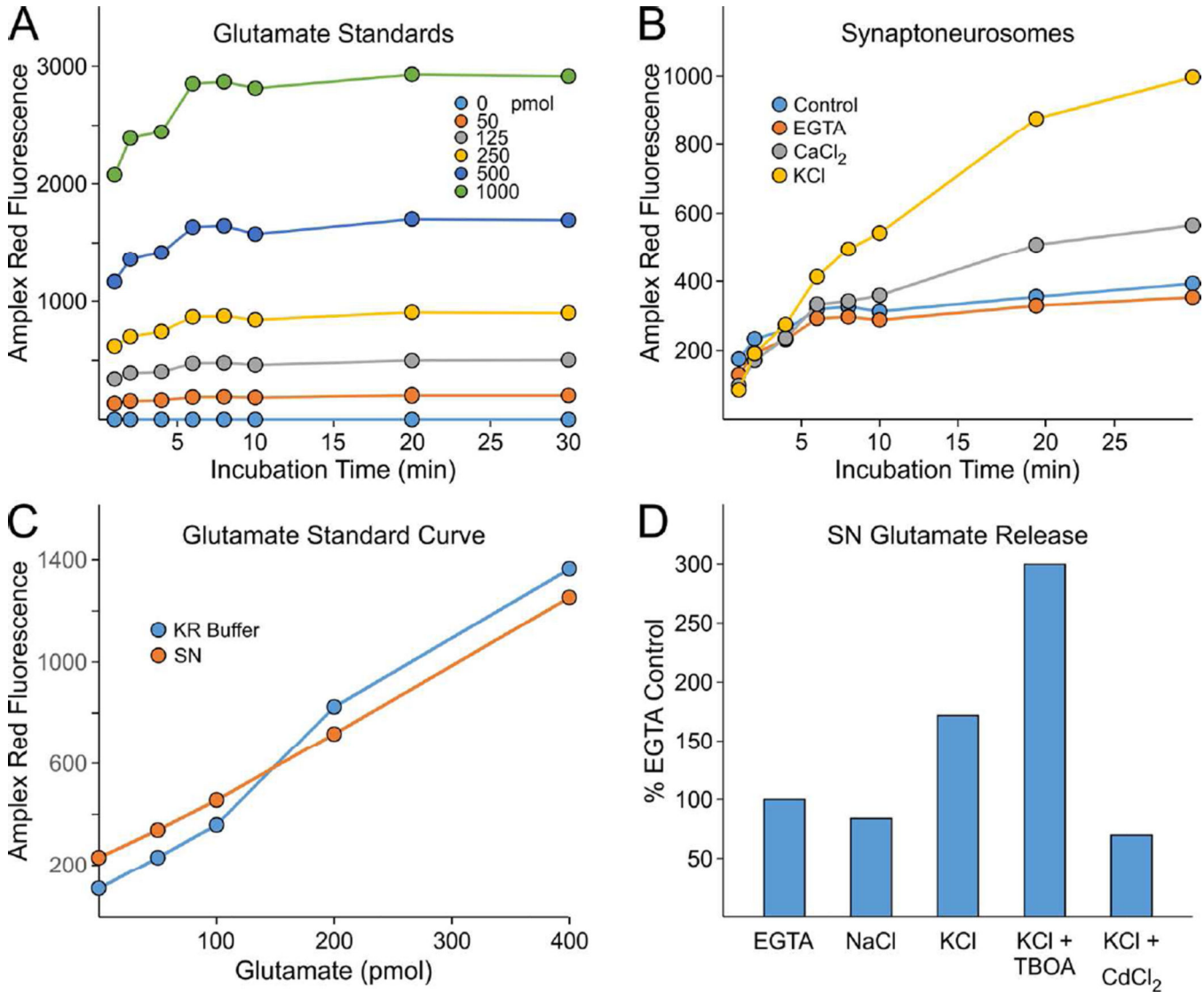

Figure 2. Characterization of SN glutamate release assay

A. Relative increase in Amplex Red fluorescence was measured in response to increasing concentrations (pmol) of glutamate standards over 30 minute time interval **B**. Enhanced fluorescence was observed for WT forebrain SNs over 30 minutes in response to both 0.5 mM $CaCl_2$ and 40 mM KCl; baseline values were observed for both H_2O control (con) and EGTA (2 mM) **C**. Glutamate standard curves in the presence of SNs were unaltered relative to KR buffer alone **D**. Depolarization-dependent (KCl)(with Ca^{2+}) glutamate release in SNs was enhanced by glutamate transporter inhibition (100 μM TBOA) but not by $CdCl_2$ (2 mM) as % of EGTA control; NaCl (40 mM) had no effect above control, ruling out osmotic effects of KCl. The same general results were obtained in separate experiments with two additional sets of WT mouse SNs.

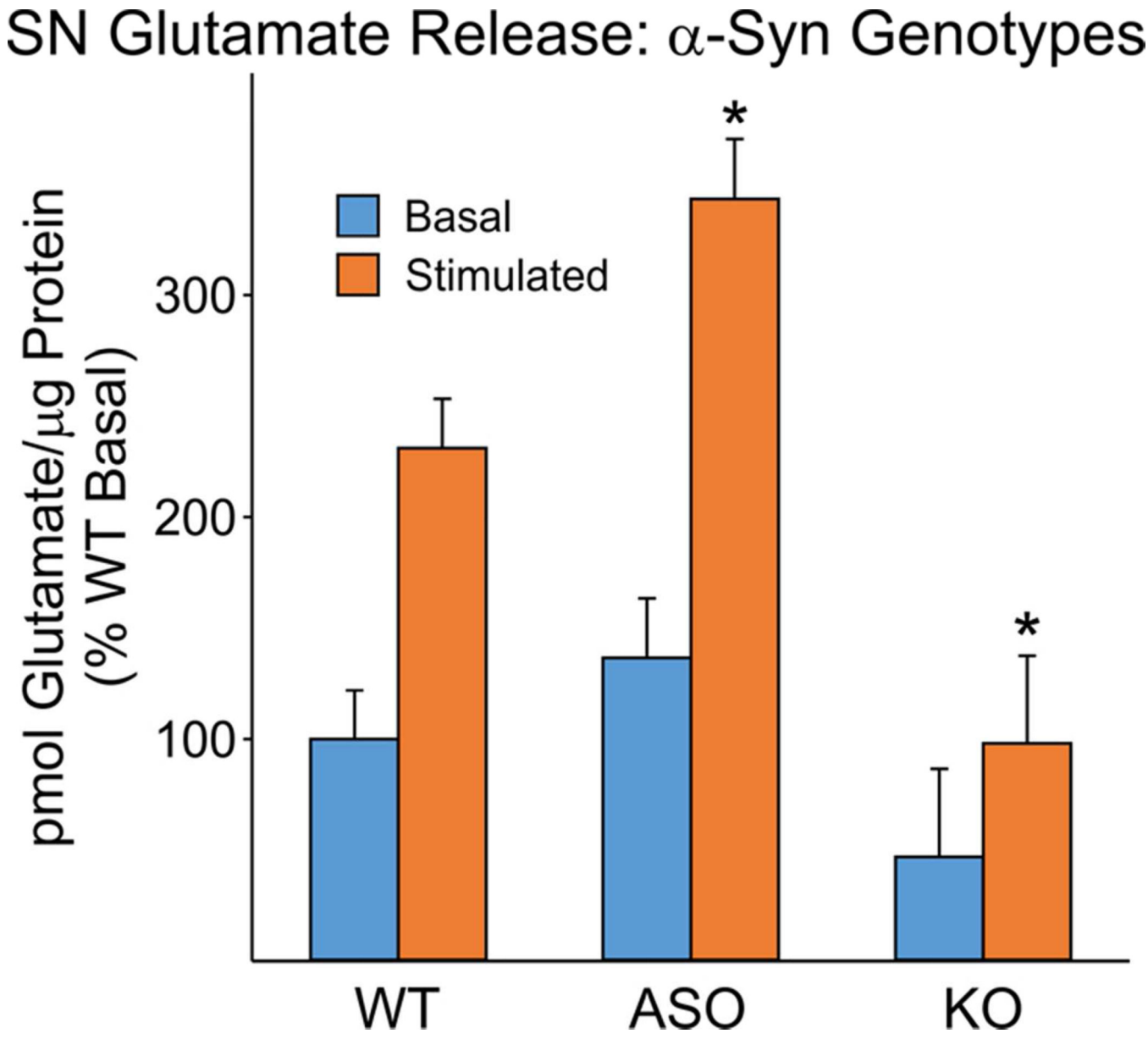

Figure 3. Effect of α-Syn mouse genotype on SN glutamate release

Glutamate values (picomoles glutamate/µg protein, % of WT basal control) were elevated in ASOTg SNs, while KO values were significantly diminished (WT, N=32 mice; ASOTg, N=22 mice; KO, N=10 mice). Values obtained from a single mouse of each genotype corresponded to a single experiment. For genotype comparisons, data was normalized to % of an absolute average basal value obtained for all WT mice (0.92+0.14 pmol glutamate/µg protein). Two Way ANOVA plus Holm-Sidak post-hoc analyses were significantly different for pairwise genotype comparisons relative to WT [*P<0.05, ASO vs WT, Difference of means (DFM) = 0.75, t=3.02; KO vs WT, DFM=.93, t=2.893] and between genotypes (P<0.05, ASO vs. KO, DFM = 1.67, t=4.95). ASO and KO stimulated values were also significantly different when compared separately with WT values (P<0.05, paired *t*-test).

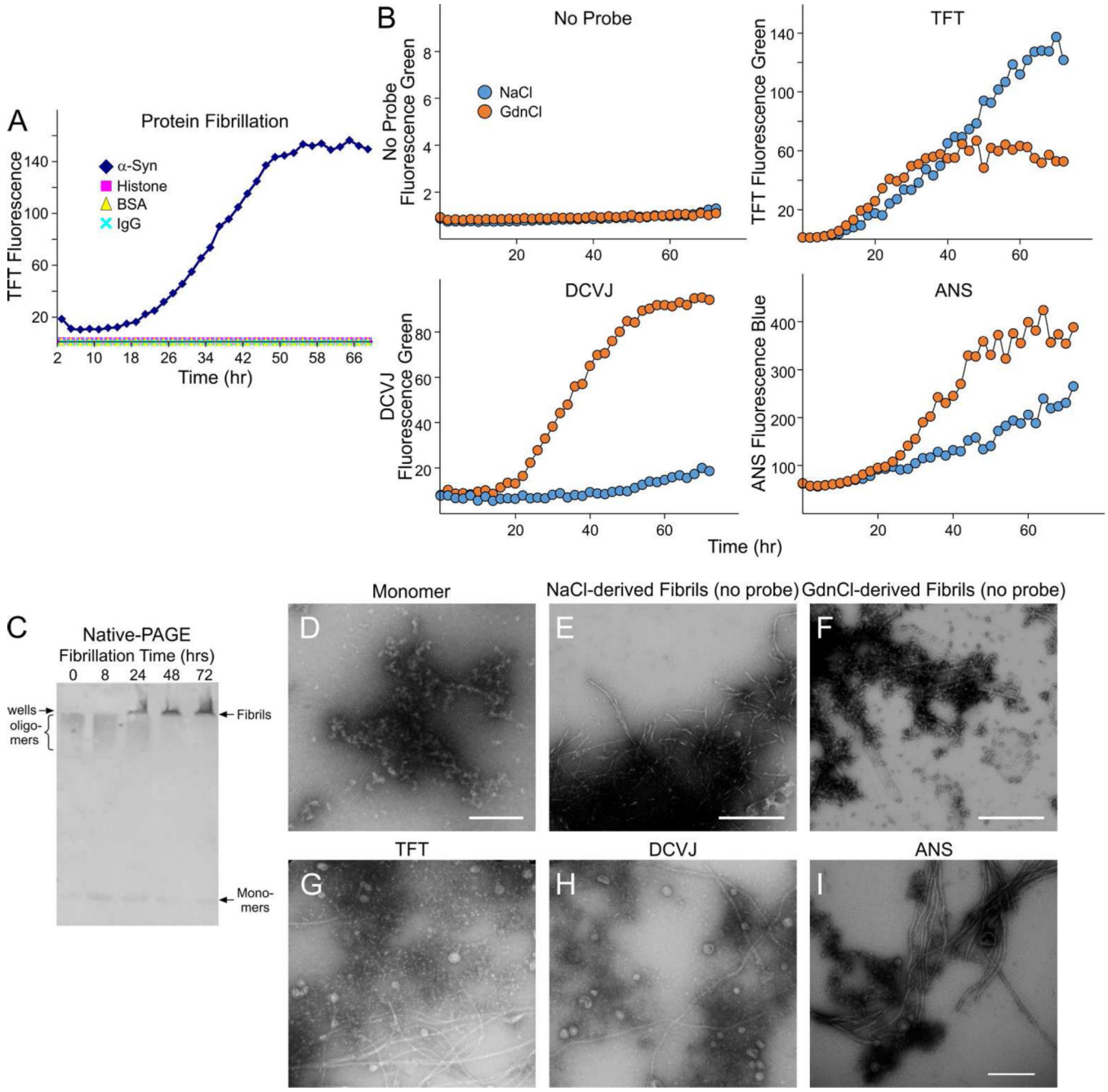

Figure 4. Fibrillation of native, full-length α-Syn

A. Fibrillation of human native, full-length α-Syn was monitored over a 72 hour time course by TFT fluorescence relative to non-aggregated control proteins (histone, BSA, IgG). **B**. Fibrillation of full-length α-Syn was performed with either NaCl (100 mM) or GdnCl (100 mM) and monitored with TFT, DCVJ, or ANS as fluorescent probes (top right, bottom panels). Differential fibrillation patterns raised the possibility of preferential binding of NaCl-derived fibrils to TFT, while GdnCl-derived fibrils showed preferential binding to DCVJ and ANS possibly due to oligomer-enrichment. **C**. Native-PAGE/immunoblotting: Native, full-length monomers and large aggregates (likely fibrils in wells) and possible

oligomers (just below wells) of α-Syn obtained using GdnCl were detected by Native-PAGE using a rabbit polyclonal anti α-synuclein antibody (1:10,000). **D**. TEM micrographs show monomers alone, NaCl-derived fibrils (**E**) or GdnCl-derived fibrils (**F**) in the absence of fluorescent probes. Additional TEM micrographs show fibrillated α-Syn using TFT, DCVJ, and ANS as fluorescent probes (G-I). Fibrils were represented by strands while structures reminiscent of oligomers were represented as circular globules (scale bars = 0.5 μm).

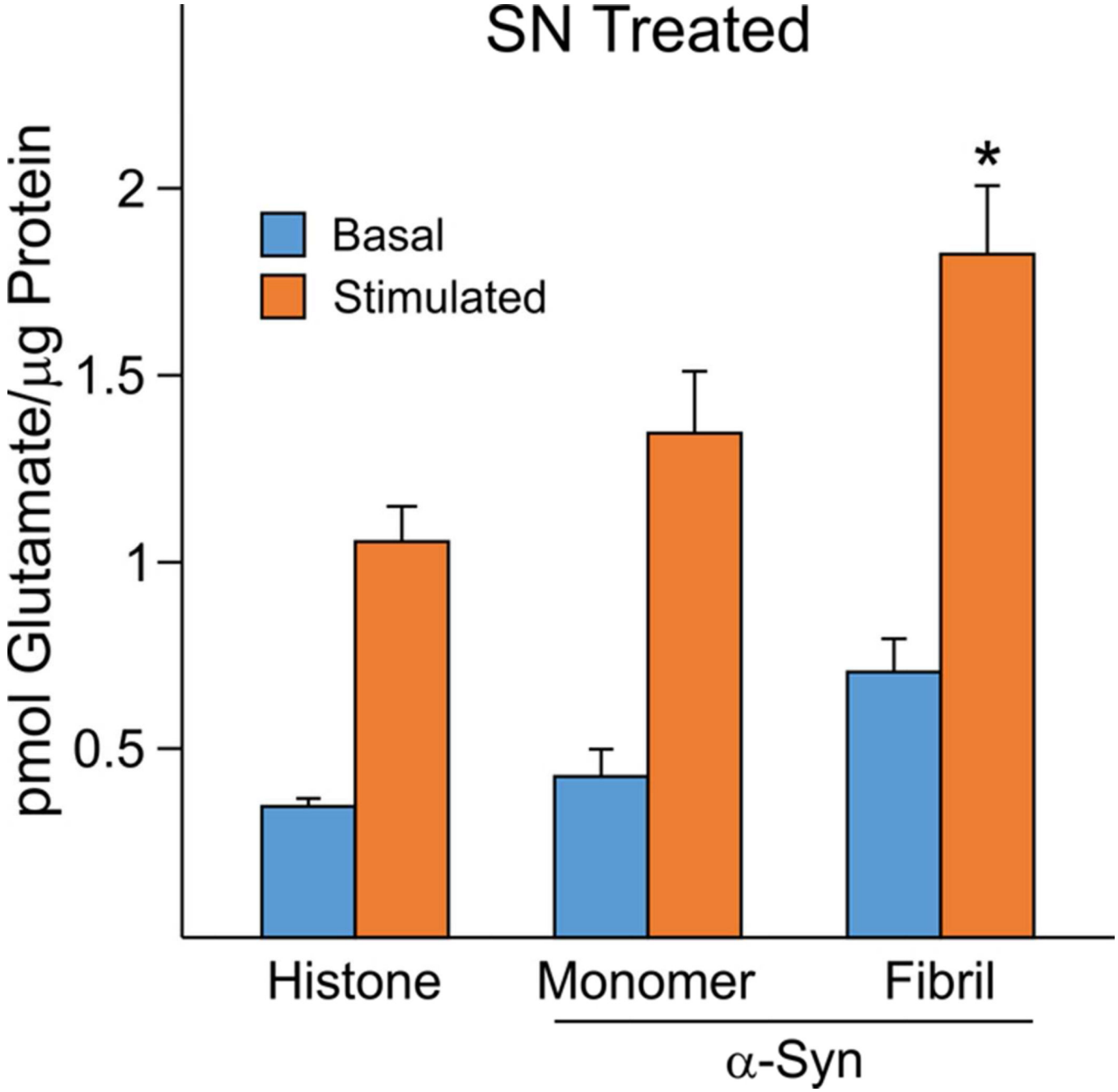

Figure 5. Enhancement of SN glutamate release by exogenous fibrillated α-Syn

A. Stimulated but not baseline WT SN glutamate release was significantly enhanced by exogenous addition (SN Treated) of fibrillated native α-Syn (NaCl-derived) (pmol glutamate released per µg protein, mean±SEM: histone control, 1.06±0.09, N=6 experiments, 4 mice; native α-Syn monomer, 1.35±0.161, N=8 experiments, 4 mice; α-Syn fibril, 1.80±0.18, N=8 experiments, 4 mice). TwoWay ANOVA and Holm-Sidak Method pairwise comparisons were used for post-hoc analyses of stimulated values for fibril vs histone and fibril vs monomer (*P<0.05).

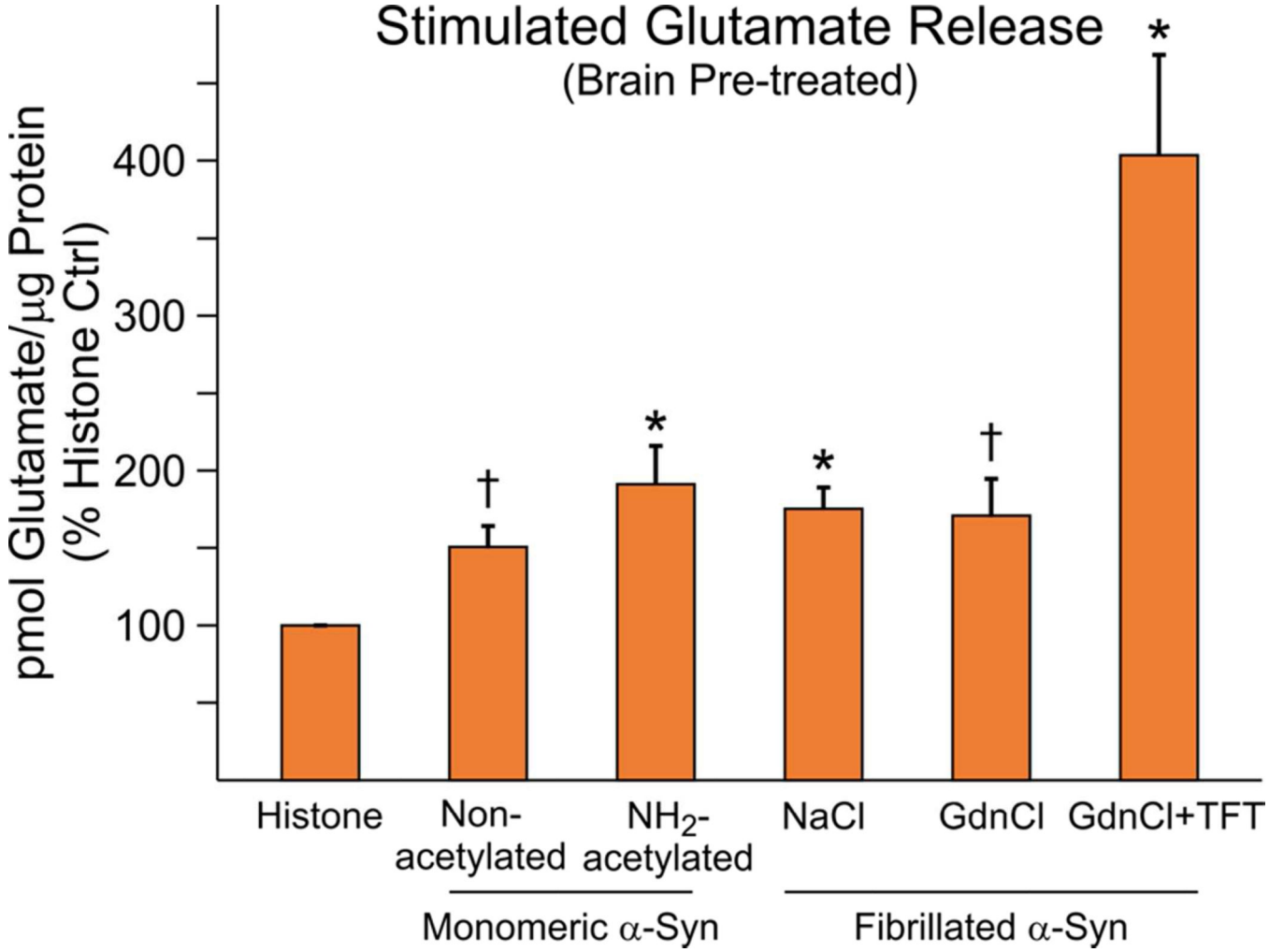

Figure 6. Enhancement of glutamate release by SN internalization with both monomeric and fibrillated α-Syn

Stimulated WT SN glutamate release was increased by both native (N=14) and NH_2-terminally acetylated forms (N=12) of monomeric α-Syn relative to % of a histone control (N=22)(10 mice were used for all experiments). Similarly all fibrillated forms (NaCl, N=12; GdnCl, N=8 GdnCl + TFT, N=4) also enhanced release ($P<0.001$, Kruskal-Wallis one way ANOVA on Ranks). NH_2-terminally acetylated, monomeric α-Syn and the NaCl-derived fibrils and GdnCl + TFT-derived fibrils were significant vs. histone control (*$P<0.05$, Pairwise Multiple Comparisons by Dunn's Method). GdnCl-derived fibrils and the native non-acetylated monomeric form were also significantly different when compared alone to the histone control (†$P<0.05$, Student paired *t*-test).

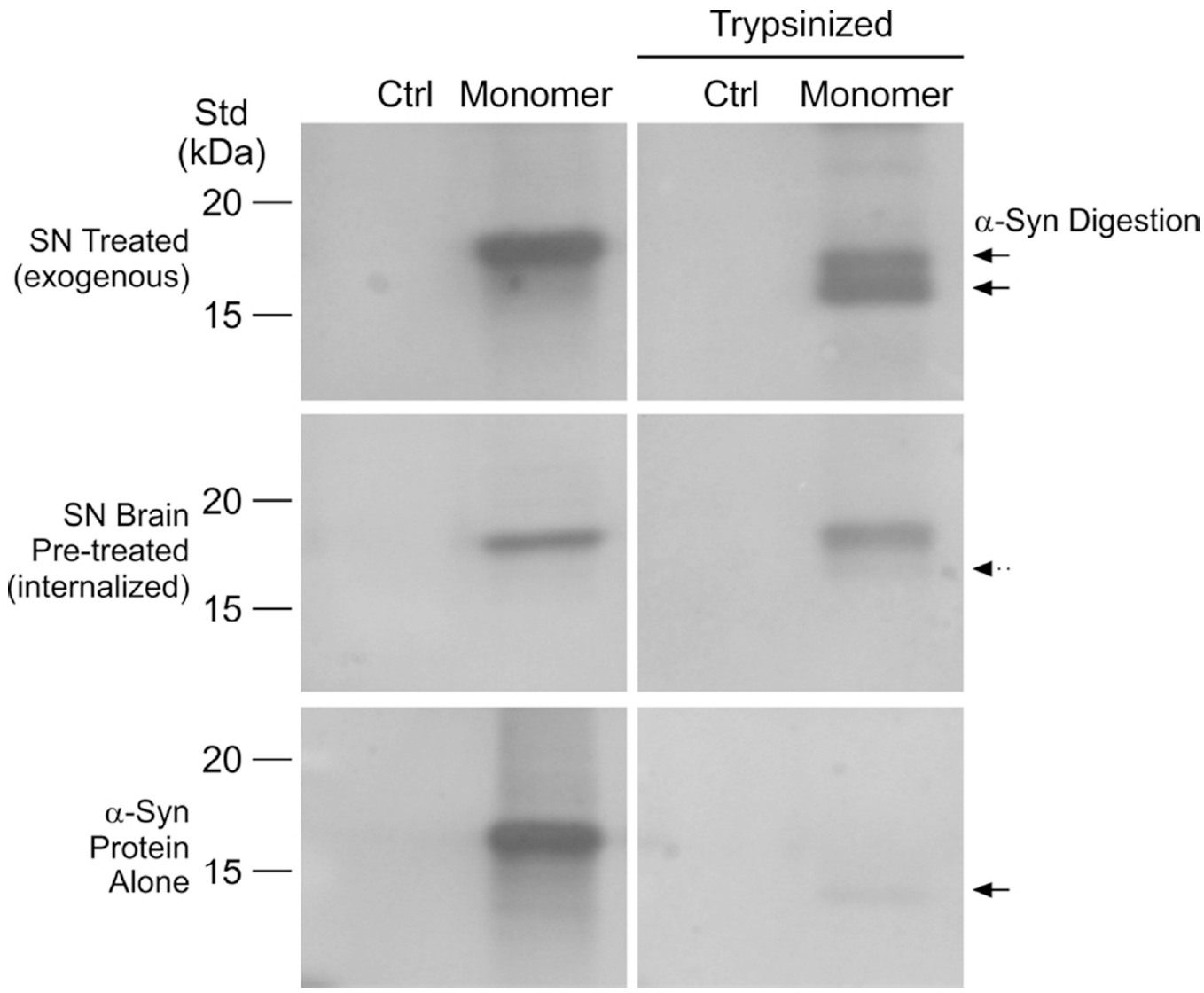

Figure 7. Trypsin-resistance of SN-internalized α-synuclein

Full-length, native monomeric α-synuclein protein (Monomer lanes) were either added exogenously after the final SN fraction (SN Treated, top panels) or added to the initial homogenization prior to SN fractionation (Brain-Pre-treated, middle panels). The use of SNs prepared from KO mice (control lanes, Ctrl) eliminated interference from endogenous mouse synuclein. SNs were either untreated (left panels) or treated with trypsin (right panels) and resolved by SDS-PAGE and Western immunoblotting (mouse monoclonal anti-α-synuclein, 1:2000). Full-length monomers were resolved as single 15–16 kDa immunoreactive bands in untreated SNs. There were relative degrees of α-synuclein (αSyn) protease digestion in trypsin-treated samples for each SN condition (SN Treated vs Brain Pre-Treated). Solid arrows denote protein bands due to trypsin digestion; dashed arrow denotes partial digestion. The α-synuclein protein alone served as a positive control for maximal trypsin digestion (bottom panel). Similar qualitative protein banding-patterns of digestion were observed in a second set of experiments. Molecular weight standards (15 kDa, 20 kDa) are denoted.

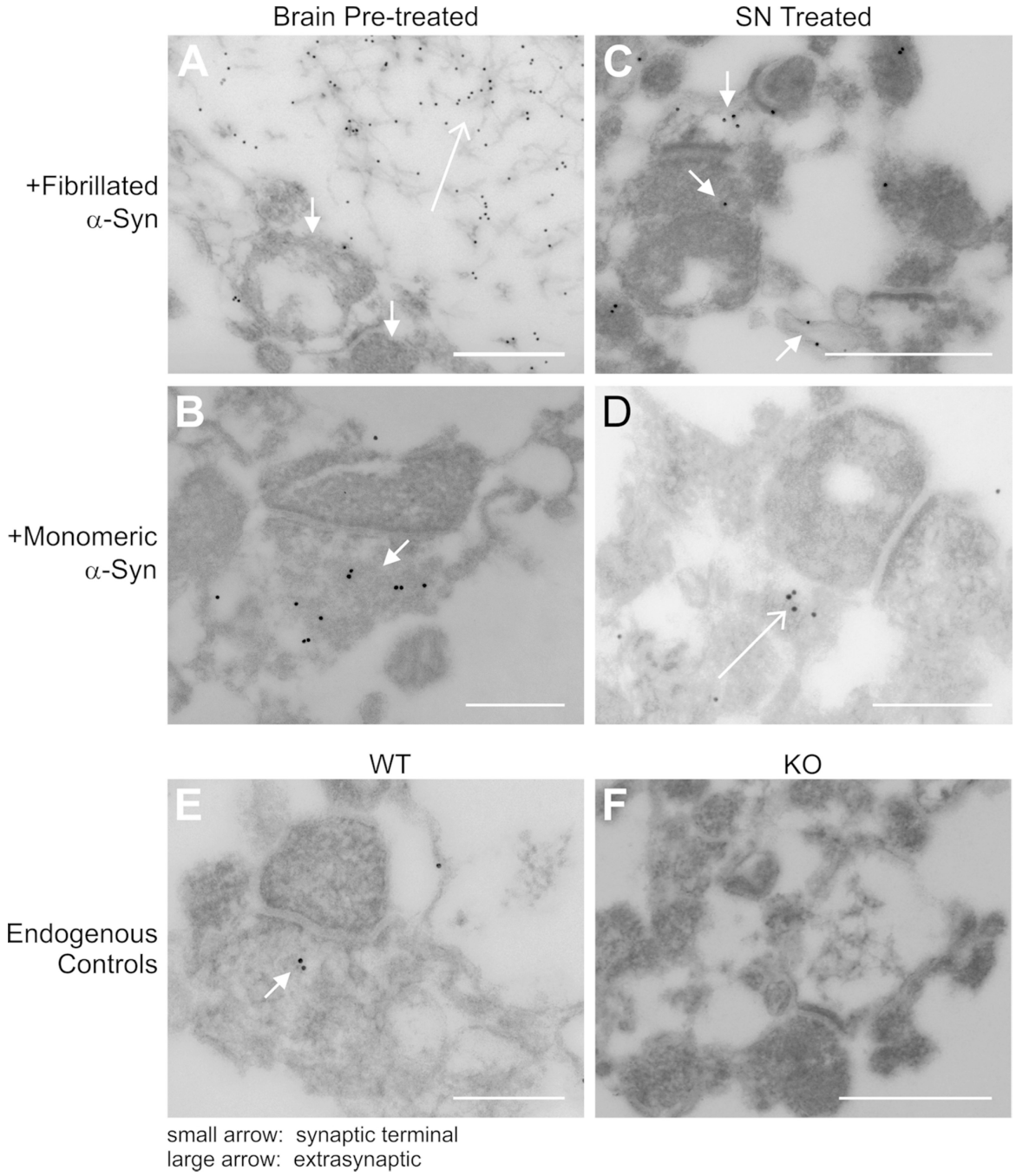

Figure 8. Association of exogenous fibrillated α-synuclein with SN membranous structures including synaptic terminals

Immuno-gold TEM detected fibrillated α-Syn (**A**) in pre-incubated SNs (Brain-Pre-treated) as gold particles in multiple synaptic terminals (small arrows) as well as intact extrasynaptic fibrils (large arrow). Labeled monomeric forms (**B**) were also found in synaptic terminals when pre-incubated with SNs. **C**. Gold-labeling was detected in synaptic terminals in mature SNs exposed to exogenous fibrillated α-Syn (small arrows). The exogenous monomeric form was found mainly outside synaptic terminals (large arrow)(**D**) Endogenous labeling in

WT SNs (**E**) and KO SNs (**F**) served as positive and negative controls respectively (panels **A–D, F**, scale bar = 0.5 μm; panel **E**, scale bar = 0.25μm).

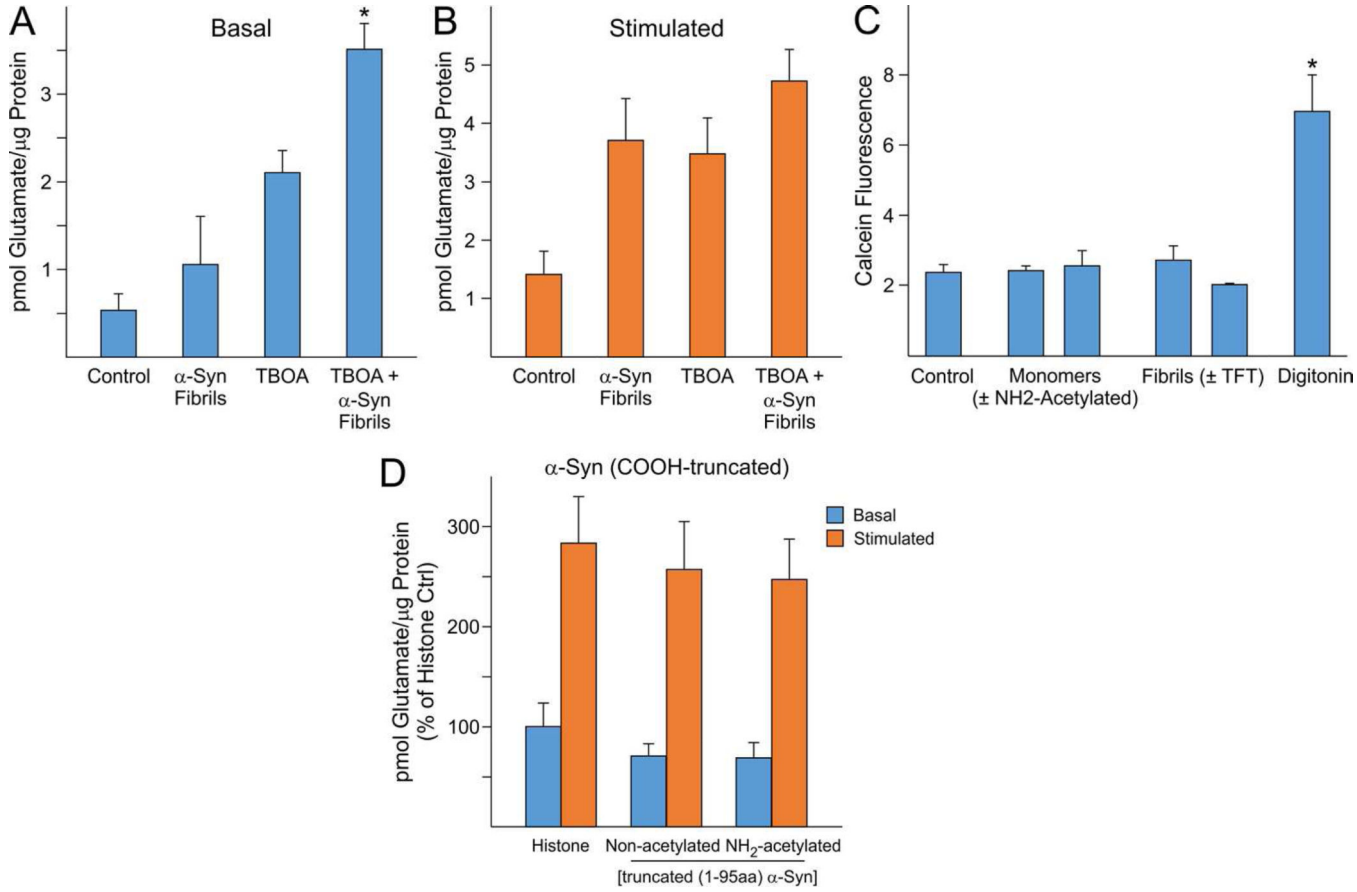

Figure 9. Exogenous fibrillated α-Syn had no measurable effect on glutamate transporter re-uptake or membrane permeabilization

A. Relative to control, TBOA alone and TBOA + fibrillated forms (α-Syn fibrils) increased basal WT SN glutamate release (control 0.535±0.19, N=4; α-Syn fibrils 1.06±0.55, N=4 mice; TBOA 2.10±0.25, N=9, 4 mice; α-Syn fibrils + TBOA 3.51±0.30, N=9, 4 mice) ($P<0.001$, One Way ANOVA; *$P<0.05$, Bonferroni *t*-test for TBOA + fibrils relative to fibrils alone. **B**. Similar TBOA treatments also enhanced levels of stimulated SN glutamate release but were not significant (control 1.42±0.40; α-Syn fibrils 3.71±0.72; TBOA 3.36±0.42; α-Syn fibrils + TBOA 5.0±0.37)($P=0.032$, One Way ANOVA, $P>0.05$ for post-hoc Bonferroni *t*-tests). TFT was present in some fibrillated α-Syn samples, but did not alter relative comparisons between groups when TBOA was added. **C**. Membrane permeabilization: A calcein release assay was used to measure pore formation in mature SNs pre-loaded with calcein and exposed to buffer alone (control), monomeric α-Syn (monomers ± NH_2-terminal acetylated), or fibrillated α-Syn (fibrils ± TFT) (N=4, 1 mouse). Only digitonin (positive control) values were significantly different than control values (*$P<0.05$, One Way ANOVA, post-hoc Dunn's Method for digitonin; also $P<0.016$, Mann-Whitney Rank Sum Test, digitonin vs control alone). **D**. Brain pre-treatment with truncated α-Syn: Prior internalization with both native and acetylated forms of COOH-truncated (1–95aa) α-Syn failed to enhance SN glutamate release under stimulated conditions when normalized as % of basal histone control (absolute average value = 1.46±0.21 pmol Glutamate/µg protein)

(control, 283±46.6%,, N=20, 9 mice; truncated/non-acetylated α-Syn, 257±47.3%, N=10, 5 mice; truncated/acetylated α-Syn, 247±39.7% N=4, 2 mice)(P>0.05, One Way ANOVA).